Ground Improvement vs. Pile Foundations?

Serge Varaksin
Apageo, France, s.varaksin@apageo.com

Babak Hamidi
GFWA, Australia, b.hamidi@gfwa.com.au

Noël Huybrechts
Belgian Building Research Institute - BBRI and KU Leuven, Belgium, nh@bbri.be

Nicolas Denies
Belgian Building Research Institute - BBRI, Belgium, nde@bbri.be

ABSTRACT

A current trend on the European market is the use of ground improvement concepts as alternative or in complement with deep foundations realized by piling methods. Several ground improvement techniques include the use of rigid inclusions. Their construction process, sometimes similar to the typical piling techniques, makes it difficult to draw a boundary between deep foundation by piles and ground improvement by rigid inclusions. In practice, this lack of clarity can lead to severe discussions between the stakeholders of the construction project and sometimes results in a feeling of double standard politics on the market of foundation contractors with severe specifications for piling contractors and nebulous requirements for ground improvement contractors. This wrong debate is generally caused by a misuse of the foundation engineering terminology and by a confusion of the roles and the failure mechanisms related to the different foundation concepts.

In the present keynote, the concept of rigid inclusions, including the use of a load transfer platform, is reviewed and illustrated with several case studies. Design methodologies, in line with the Eurocodes, are discussed and promoted in order to ensure a positive competition or a strong collaboration between both worlds. The authors give a general overview of the rigid inclusion concept including theoretical, design and execution aspects. Recent trends on the market (deep mixing, CMC…) are highlighted and research perspectives proposed to further understand the fundamental principles governing the different foundation concepts.

1. INTRODUCTION

1.1. Ground Improvement vs. Foundation Piles – the wrong debate

A current trend on the European market, as all over the world, is the use of ground improvement concepts as alternative to or in complement with deep foundations installed with typical piling methods. The Belgian market is no exception to the rule. If the design of foundation piles to transmit the structural loads to the ground is now well established - notably with the development of the Eurocodes and their National Annexes - the way to design ground improvement concepts still remains unclear. This absence of design rules is sometimes considered as an advantage for the use of ground improvement methods as lesser rules equate to lesser constraints and lesser design requirements and control (values). Nevertheless, most of the time, this lack of design rules leads to severe, long and expensive discussions sometimes resulting in the elimination of the ground improvement solution only due to the lack of clarity of the design framework of the concept. This elimination can cost much for all the parties involved in the project. In European countries - where the design of the engineering solutions is more and more established under the umbrella of the EN standards - the lack of design rules for ground improvement concepts really represents an obstacle to the growth of this kind of alternative solution.

A practical example is the replacement of foundation piles by a concept of ground improvement involving soil mix elements. When we begin to compare both solutions, it is always the beginning of an irrelevant debate with the following questions: *"how to conform the soil mix elements to the severe requirements imposed to concrete piles on the market"?* or *"Are the soil mix elements in agreement with the requirements of Eurocode 7 for the piles"?* In this way of thinking, the soil mix element (which can be a column or a rectangular panel) is directly considered as a pile of lower quality, a cheap pile or a "second-hand" pile. Indeed, how to compare a well-known concept (reinforced concrete pile or steel pile) supported by EN

design requirements (Eurocode 7 and National Annexes, e.g. Rapport 12 of BBRI in Belgium) and European (CE) and local (e.g. Benor in Belgium) material markings with a foundation concept including soil mix elements made of a mix of grout and soil (in the deep mixing process, the ground is mechanically mixed in place, while a binder, often based on cement, is injected). Finally, if the ground improvement concept involving soil mix elements is still selected in place of the pile foundation solution, there is always the same reaction from the concrete industry and the piling contractors highlighting the unbalanced design requirements for soil mix elements and concrete products and the unfair competition between both techniques. *"Why do we have to conform to severe (and costly) QA/QC rules for well-known and recognized technique and material while, when we work with an innovative technique such as the deep mixing, the requirements are more flexible (or sometimes do not exist)"?* There is thus a feeling of double standard politics on the market of foundation contractors.

Actually, this is a wrong debate. And this latter is caused by the idea that a "soil mix element" can be a "soil mix pile". In order to close the debate, it is really important to avoid this terminology. A soil mix element is not a pile. In the United States of America, for example, the terms used are "soil-cement columns" or "soil mix panels" but reference is not made to "soil mix piles". In reality, we are dealing with different geotechnical concepts. In the classical piling concept, the foundation pile is used to transmit the structural loads to deeper rock or firm soil layers (= base resistance) at sites presenting soft/weak/compressible soils at shallow depths and to support loads by shaft resistance (= skin friction). The resistance of the soft soil located under the concrete slab is generally not considered in the design, which is not always the case with the ground improvement concepts. In order to fully understand the issue, it is necessary to return to the roots of foundation engineering.

1.2. Behind the geotechnical concepts – back to the roots

Commonly it is envisaged that shallow footings directly rest on competent ground, and deep foundations are used to transfer loads to deep firm ground. According to Salgado (2008):

- "*Shallow foundations transfer structural loads to relatively small depths into the ground. They range from isolated foundations, each carrying its own column load, to elements carrying several columns, walls or even all the loads for a given structure or building".*
- *"Piles are long, slender elements made of concrete, steel, timber, or polymer used to support structural loads. Historically, piles have been used to transfer structural loads to deeper rock or firm soil layers at sites where soft clays or loose sands exist at shallow depths. In recent decades, the uses expanded to absorbing tensile and lateral loads, to supporting loads by shaft resistance, and to reducing the settlement of mat foundations*".

In other references, limitations are introduced in the definitions considering the dimensions of the different foundation elements. Terzaghi et al. (1996) define a shallow footing as a footing that has a width equal to or greater than the foundation depth, which is the distance from the level of the ground surface to the base of the footing, and a pile as a very slender pier that transfers a load through its lower end onto a firm stratum or else through side friction onto the surrounding soil. Bowles (1996) defines shallow foundations as bases, footings, spread footings or mats with the ratio of depth of footing to its width being equal to or less than 1, and defines deep foundations as piles, drilled piers or caisson with ratio of length to width (or diameter) being equal to or greater than 4. Das (2009) notes that studies show that the ratio of footing depth to width of shallow footings can be as large as 3 or 4.

While it is very beneficial to have concise definitions for various concepts and behaviors to avoid confusion and to facilitate the accurate transfer of thoughts and intent, it can be observed that it is not possible to simply set an integer as the separation point between the two foundation systems and more insight into the matter may be required. These two terms are only a simplification for explaining the mechanisms of load transfer to the ground. Bearing of shallow foundations are generally expressed by shear theories originally developed by Prandtl (1920), Terzaghi (1943), Meyerhof (1951) and Hansen (1971). Skin resistance (Tomlinson, 1971; Vijayvergiya and Focht, 1972 and Burland, 1973) may become a major contributor as the ratio of footing height to width begins to increase. At the same time, while a large based footing may be categorised as a shallow foundation system due to its ratio of depth to width, the depth of soil within the system may be very deep indeed. Hence, the distinction between both foundations concepts (shallow or deep) is not always easy to achieve. This topic will later be discussed in the present keynote.

Moreover, a pile is rarely used alone. The structural loads are often transmitted to the ground with the help of pile groups involving the consideration of the group effect in the design. In a pile group, the loads are transmitted to the ground only via the piles, which are linked together by a pile cap. Even if the pile cap is in practice in contact with the soil, it is not included in the calculation of the bearing capacity. That is not

the case with a pile raft. In a pile raft, the piles and the raft foundation are designed together in order to reduce potential settlement of the structure. The percentage of the load taken by the slab of the piled raft solution is normally far more than the load taken by the pile cap of a pile group where only the piles are responsible of the load transfer. Pile raft is thus a concept often used in a Serviceability Limit States (SLS) logic.

To further complicate this simple categorization, it is also possible to convert deep loose or soft soils to adequately competent soil by ground improvement; thereby safely dissipating the loads without engaging piles for transferring loads to deeper firm ground.

During the last decades, the importance of the ground improvement market has enormously increased. New methods, tools and procedures have been developed and applied in practice. A particularity of this field of geotechnical engineering is that a major part of the advances in ground improvement has to be credited to the equipment manufacturers and to the specialist contractors. If this constant improvement of the technologies stretches the boundaries of the practical applications, it sometimes results in a lack of theoretical concept background to support these applications on the market. Theory and design aspects do not follow fast enough to support these technological developments and their resulting applications. As a consequence, geotechnical designers are often exposed to new execution processes without enough information to support the geotechnical concepts behind the proposed applications.

A first issue is the number of ground improvement methods available on the international market. In order to answer this question, the ISSMGE Technical Committee TC 211 (former TC17) has adopted a classification system, shown in Table 1, with the following categories (and methods) for ground improvement works:

- Category A: Ground Improvement without admixtures in non-cohesive soils or fill materials (dynamic compaction, vibrocompaction…)
- Category B: Ground Improvement without admixtures in cohesive soils (Replacement, preloading, vertical drains, vacuum consolidation…)
- Category C. Ground Improvement with admixtures or inclusions (Vibro replacement - stone columns, sand compaction piles, rigid inclusions…)
- Category D. Ground Improvement with grouting type admixtures (Particulate and chemical grouting, Deep mixing, jet grouting…)
- Category E. Earth reinforcement (Geosynthetics or MSE, ground anchors, soil nails…)

This classification is based on the broad trend of behaviors of grounds to be improved and whether admixtures are used or not. Chu et al. (2009) have classified and described the various ground improvement techniques that are commonly practiced to date. It is not possible to mention all techniques in this paper; however, separate lists are given on the ISSMGE TC211 website (www.tc211.be).

Some of these techniques are developed to improve the physical and mechanical properties of *in-situ* soils without the introduction of imported material, and the outcome will remain as what is classically referred to as a shallow foundation (e.g. preloading with vertical drains, dynamic consolidation, etc.).

In other ground improvement techniques, higher quality materials are added to the ground as columnar inclusions. Some inclusions may be very long and can call pile foundations to mind. Nevertheless, in these geotechnical concepts, foundations are made of classical shallow footings combined with (deep) soil masses that have been improved by the installation of the inclusions. These foundations cannot be expressed by the classical shallow foundation approaches as reported in the previous paragraph, and require further analysis and design of the improved ground as part of the foundation system. The complication in the categorisation can turn into confusion when columnar inclusions are formed by installing concrete and grout columns in the ground using piling equipment. That uncertainty particularly concerns the installation of rigid inclusions (category C5) and the use of soil mix elements (D3) as alternatives to typical pile foundations.

As defined in Chu et al. (2009), rigid inclusions refer to the use of semi-rigid or rigid integrated columns or bodies in soft ground to improve the ground performance globally so as to decrease settlement and increase the bearing capacity of the ground. In the broad sense, the concept of stone columns is a type of rigid inclusions. However, they are not considered because the materials used for those columns (generally crushed stones) are disintegrated and the columns formed in the ground are not able to stand without the lateral support of the soil. Contrarily, the constitutive material of the rigid inclusions is continuous and presents a high permanent cohesion. Its rigidity is therefore higher than the rigidity of the surrounding soil. Typical rigid inclusions are concrete columns (possibly installed into the ground with a classical piling technique), grout columns, soil mix elements (columns, panels, trenches, blocks, etc.), Controlled Modulus Columns (CMCs), grouted stone columns, etc.

Table 1. Classification of ground improvement methods of the ISSMGE TC211 (from Chu et al., 2009)

Category	Method	Principle
A. Ground improvement without admixtures in non-cohesive soils or fill materials	A1. Dynamic compaction	Densification of granular soil by dropping a heavy weight from air onto ground.
	A2. Vibrocompaction	Densification of granular soil using a vibratory probe inserted into ground.
	A3. Explosive compaction	Shock waves and vibrations are generated by blasting to cause granular soil ground to settle through liquefaction or compaction.
	A4. Electric pulse compaction	Densification of granular soil using the shock waves and energy generated by electric pulse under ultra-high voltage.
	A5. Surface compaction (including rapid impact compaction).	Compaction of fill or ground at the surface or shallow depth using a variety of compaction machines.
B. Ground improvement without admixtures in cohesive soils	B1. Replacement/displacement (including load reduction using lightweight materials)	Remove bad soil by excavation or displacement and replace it by good soil or rocks. Some lightweight materials may be used as backfill to reduce the load or earth pressure.
	B2. Preloading using fill (including the use of vertical drains)	Fill is applied and removed to pre-consolidate compressible soil so that its compressibility will be much reduced when future loads are applied.
	B3. Preloading using vacuum (including combined fill and vacuum)	Vacuum pressure of up to 90 kPa is used to pre-consolidate compressible soil so that its compressibility will be much reduced when future loads are applied.
	B4. Dynamic consolidation with enhanced drainage (including the use of vacuum)	Similar to dynamic compaction except vertical or horizontal drains (or together with vacuum) are used to dissipate pore pressures generated in soil during compaction.
	B5. Electro-osmosis or electro-kinetic consolidation	DC current causes water in soil or solutions to flow from anodes to cathodes which are installed in soil.
	B6. Thermal stabilisation using heating or freezing	Change the physical or mechanical properties of soil permanently or temporarily by heating or freezing the soil.
	B7. Hydro-blasting compaction	Collapsible soil (loess) is compacted by a combined wetting and deep explosion action along a borehole.
C. Ground improvement with admixtures or inclusions	C1. Vibro replacement or stone columns	Hole jetted into soft, fine-grained soil and back filled with densely compacted gravel or sand to form columns.
	C2. Dynamic replacement	Aggregates are driven into soil by high energy dynamic impact to form columns. The backfill can be either sand, gravel, stones or demolition debris.
	C3. Sand compaction piles	Sand is fed into ground through a casing pipe and compacted by either vibration, dynamic impact, or static excitation to form columns.
	C4. Geotextile confined columns	Sand is fed into a closed bottom geotextile lined cylindrical hole to form a column.
	C5. **Rigid inclusions**	Use of piles, rigid or semi-rigid bodies or columns which are either premade or formed *in-situ* to strengthen soft ground.
	C6. Geosynthetic reinforced column or pile supported embankment	Use of piles, rigid or semi-rigid columns/inclusions and geosynthetic girds to enhance the stability and reduce the settlement of embankments.
	C7. Microbial methods	Use of microbial materials to modify soil to increase its strength or reduce its permeability.
	C8 Other methods	Unconventional methods, such as formation of sand piles using blasting and the use of bamboo, timber and other natural products.
D. Ground improvement with grouting type admixtures	D1. Particulate grouting	Grout granular soil or cavities or fissures in soil or rock by injecting cement or other particulate grouts to either increase the strength or reduce the permeability of soil or ground.
	D2. Chemical grouting	Solutions of two or more chemicals react in soil pores to form a gel or a solid precipitate to either increase the strength or reduce the permeability of soil or ground.
	D3. Mixing methods (including premixing or **deep mixing**)	Treat the weak soil by mixing it with cement, lime, or other binders *in-situ* using a mixing machine or before placement
	D4. Jet grouting	High speed jets at depth erode the soil and inject grout to form columns or panels
	D5. Compaction grouting	Very stiff, mortar-like grout is injected into discrete soil zones and remains in a homogenous mass so as to densify loose soil or lift settled ground.
	D6. Compensation grouting	Medium to high viscosity particulate suspensions is injected into the ground between a subsurface excavation and a structure in order to negate or reduce settlement of the structure due to ongoing excavation.
E. Earth reinforcement	E1. Geosynthetics or mechanically stabilised earth (MSE)	Use of the tensile strength of various steel or geosynthetic materials to enhance the shear strength of soil and stability of roads, foundations, embankments, slopes, or retaining walls.
	E2. Ground anchors or soil nails	Use of the tensile strength of embedded nails or anchors to enhance the stability of slopes or retaining walls.
	E3. Biological methods using vegetation	Use of the roots of vegetation for stability of slopes.

The concept behind the use of rigid inclusions is not the same as the concept of pile foundations. In the concept of rigid inclusions, the loads sustained by the soft soil is reduced (usually between 60 and 90%) in order to reduce the global and differential settlements. Nevertheless, the loads are not directly transmitted to depth. Here, the soft soil plays a role, and supports part of the load whereas in the pile foundation concept the soft soil is just bypassed (or used for skin friction consideration).

When we work with rigid inclusions, a Load Transfer Platform (LTP) is often used with a thickness generally ranging between 40 and 80 cm. In general, the load transfer platform may consist of single or multiple layers of geosynthetics (often geogrids) placed horizontally in a layer of well compacted granular material (often crushed stones or gravels). As illustrated in Fig. 1, in comparison with other commonly utilized foundation concepts, the load transfer platform allows the transfer of the structural loads to the head of the rigid inclusions by means of an arching effect developing in the granular layer. This effect is caused by the differential settlement arising between the soft soil and the heads of the rigid inclusions at the base of the load transfer platform, which also results in the emergence of a negative skin friction along the rigid inclusions at shallow depth. This negative skin friction is a governing factor of the load transfer in the concept of rigid inclusions and will be further discussed. Finally, it is to note that the installation of a load transfer platform also allows the decrease of the bending moments and the shear stresses in the foundation slab of the structure to be supported.

Previously studied by Combarieu (1988), the concept of rigid inclusions applied with a load transfer platform has more recently been the subject of an extensive French national research programme called ASIRI (*Améliorations des Sols par Inclusions Rigides*, which translates to *Ground Improvement by Rigid Inclusions*) (IREX, 2012). The following paragraphs concentrate on the main aspects of this topic.

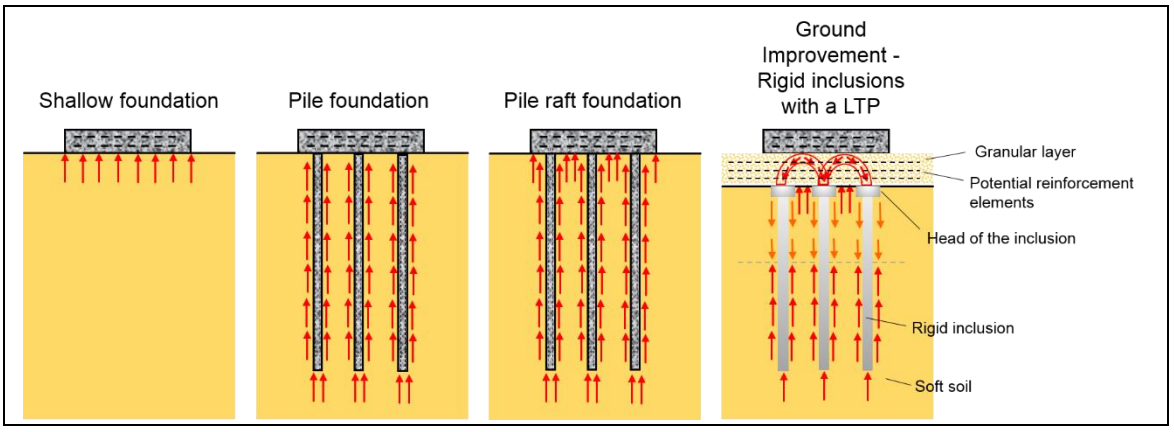

Figure 1: Type of load transfer in the different usual foundation concepts

2. CONCEPT OF GROUND IMPROVEMENT BY RIGID INCLUSIONS

2.1. Study of the mechanisms at an early stage

Combarieu (1988) has originally studied the behavior of rigid inclusions installed in soft ground. As shown in Fig. 2, a compressible soil layer of thickness H subjected to an embankment load with intensity q_o will ultimately settle an amount that can be denoted as $W_s(o)$. Likewise, the settlement at any depth, z, can be denoted by $W_s(z)$. Considering the addition of an inclusion in the engineering issue, it is interesting to focus on the settlement of both materials: the soil and the rigid inclusion. The soil conditions at distances away from the single inclusion are identical to untreated ground after complete stabilisation. However, the stress and deformations change around the immediate vicinity of the inclusion. The inclusion settles by an amount equal to $W_p(z)$ due to the loading plus a further small amount due to its own compression. Settlement is higher when the rigid inclusion terminates on soft soil (see Fig. 3) compared to when it is supported by hard soil (see Fig. 4). In the lower part of the inclusion, where $z > h_c$, the settlement of the soil is smaller than the inclusion settlement (including its compression); however, the opposite is true in the upper portion where $z < h_c$. Soil and inclusion settlements are only equal at $z = h_c$. There is thus the development of a differential settlement between the soil and the rigid inclusion, as previously stated, with the onset of a negative skin friction along the inclusion when $z > h_c$.

As shown in Fig. 5, Combarieu (1988) has also considered the equilibrium of the forces acting on the rigid inclusion. The four forces acting on the inclusion at equilibrium are:

- the driving forces: the vertical load Q acting on the head of the inclusion and the resultant negative friction, F_n, acting along the inclusion segment with a length equal to h_c.
- the resisting forces: the positive friction, F_p, mobilised in the lower part of the inclusion and along a segment with length $L - h_c$, and Q_p acting at the base of the rigid inclusion. The balance of the forces is therefore $Q + F_n = F_p + Q_p$.

According to Combarieu (1988), the computation of the bearing capacity of the rigid inclusion will be therefore influenced by the development of the negative skin friction along the inclusion.

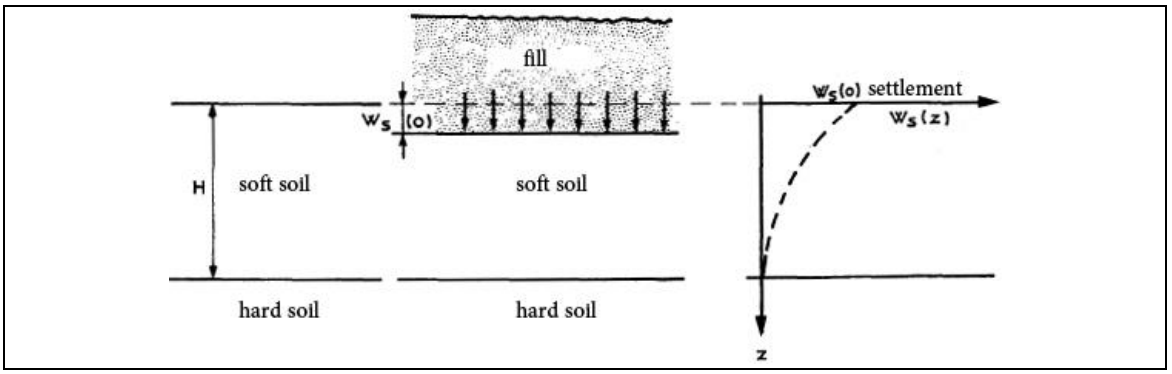

Figure 2: Ground section without rigid inclusion (Combarieu, 1988)

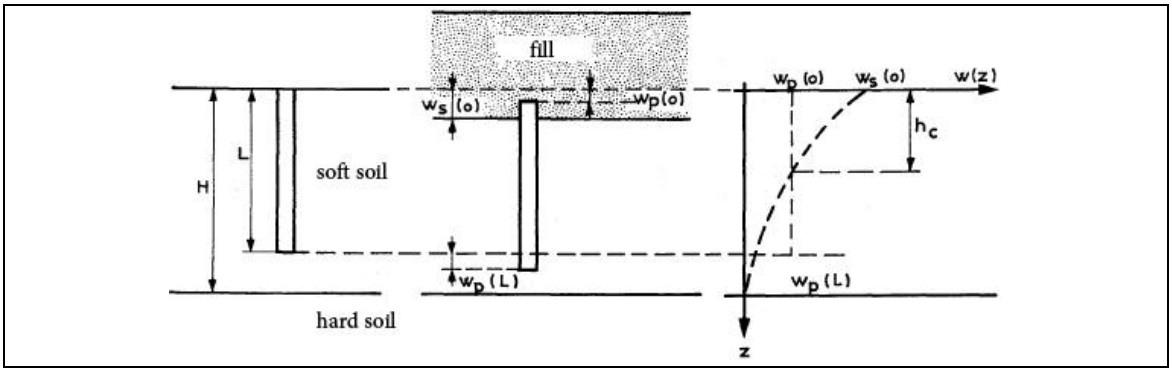

Figure 3: Ground section with rigid inclusion terminating in soft ground (Combarieu, 1988)

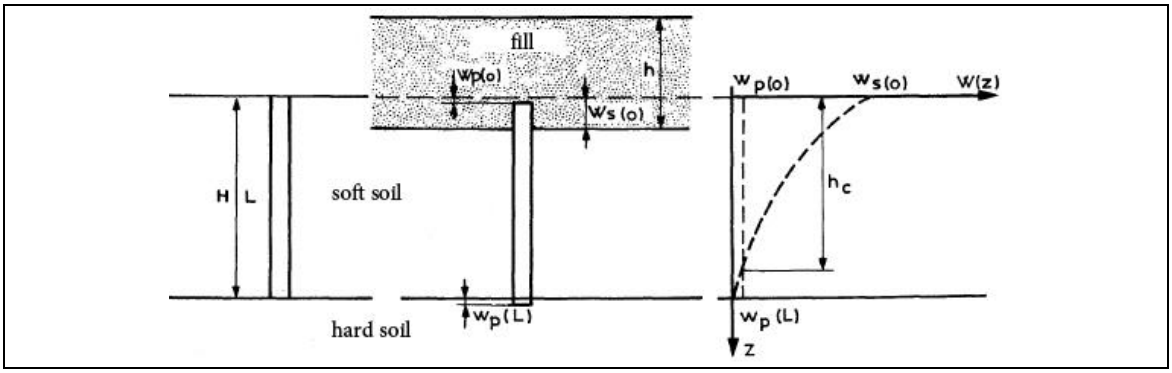

Figure 4: Ground section with rigid inclusion supported by hard ground (Combarieu, 1988)

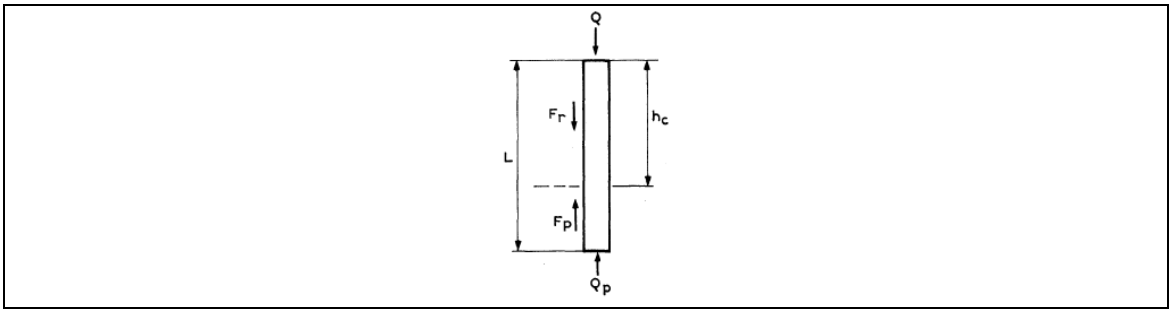

Figure 5: Forces acting on a rigid inclusion (Combarieu, 1988)

2.2. Study of the mechanisms and design approach – ASIRI project (IREX, 2012)

2.2.1. Load Transfer Platform (LTP) and failure mechanisms

As shown in Fig. 6, it is assumed that rigid inclusions, with diameter $D = 2r_p$, are installed in a square grid with centre to centre spacing, denoted by s. The thickness of the load transfer platform (LTP) is denoted by H_M, and it is defined by its characteristics (cohesion c', friction angle φ' and volumetric weight γ). The uniformly distributed external load applied to the load transfer platform is indicated by q_o.

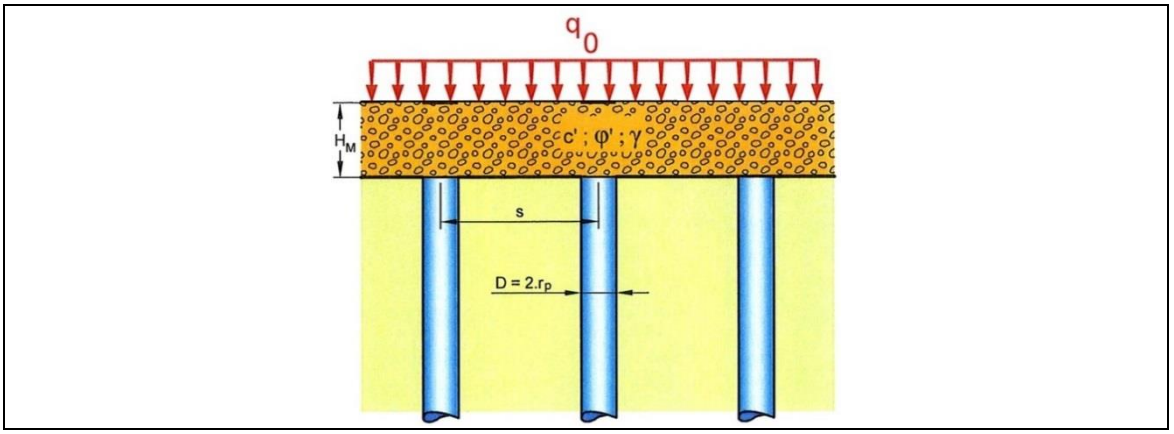

Figure 6: Cross section illustrating the concept of ground improvement by rigid inclusions, including the load transfer platform (LTP), for a uniform external loading q_0 (from IREX, 2012)

The ASIRI project (IREX, 2012) has demonstrated that two failure mechanisms are possible for that foundation concept: the Prandtl's failure mechanism and the punching shear failure mechanism.

2.2.1.1. Prandtl's failure mechanism

According to Prandtl (1920), Prandtl's failure mechanism occurs when the load transfer platform is covered by a rigid structural element (such as a slab on grade, a raft or footings) or when the embankment is sufficiently thick to avoid punching failure (which corresponds to the formation of shear cones in the LTP's surface).

According to the ASIRI guidelines (IREX, 2012), an embankment is considered thin once:

$$H_M < 0.7(s - D) \quad (1)$$

As shown in Fig. 7(a), Prandtl's failure diagram includes a Rankine active limit state domain (I) above the inclusion head, which is delimited by a logarithmic spiral arc domain (II) and a Rankine passive limit state domain (III), which is located beyond the inclusion head. q_p^+ is the stress applying on the inclusion head, and q_s^+ is the stress applying on the *in-situ* soil.

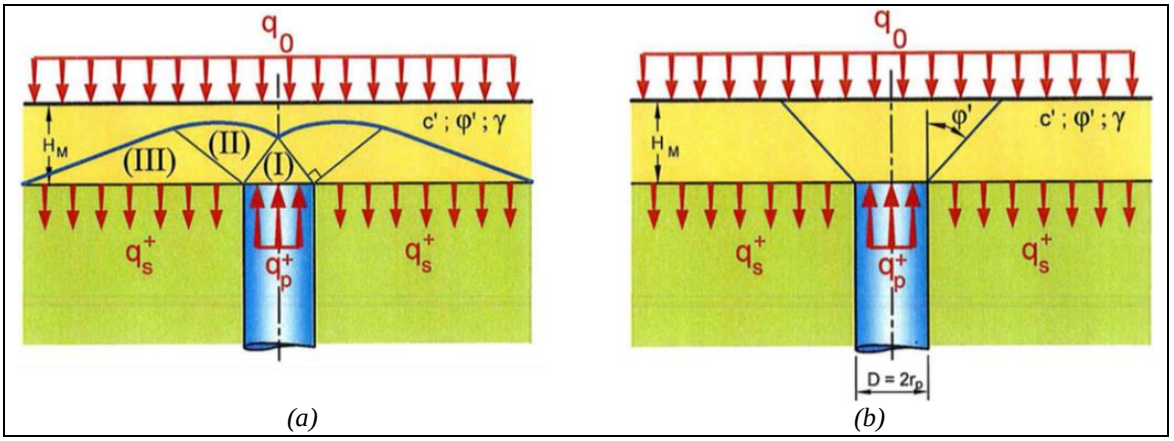

Figure 7: (a) Prandtl failure mechanism for slabs on grade, rafts, footings and thick embankments and (b) punching shear failure mechanism for thin embankments (from IREX, 2012)

The guidelines of the ASIRI project (IREX, 2012) have been developed in agreement with the philosophy of the Eurocodes. The maximum load that can be applied to the inclusion head q_p^+ is therefore calculated at the Ultimate Limit State condition (ULS). This ULS verification is performed by implementing Eurocode 7 - Design Approach 2 (EN 1997-1, 2004) with the combination of partial factors: *A1 + M1 + R2* (*A* for Action, *M* for Material and *R* for Resistance), which means that load factors on dead and live loads are respectively 1.35 and 1.50 and the partial material factors are equal to 1.

According to Prandtl's diagram, q_p^+ can be determined from the stress applied on the supporting soil and the intrinsic parameters of the load transfer platform:

$$q_p{}^+ = s_q N_q q_s{}^+ + s_c N_c \frac{c'}{\gamma_{c\prime}} - s_\gamma N_\gamma r_p \frac{\gamma}{\gamma_\gamma} \tag{2}$$

N_q, N_c and N_γ are coefficients that are functions of the friction angle of the constitutive material of the load transfer platform, and can be calculated from equations (3) to (5):

$$N_q = \tan^2\left(\frac{\pi}{4} + \frac{\frac{\varphi'}{\gamma_{\varphi\prime}}}{2}\right) \times e^{\pi \tan\left(\frac{\varphi\prime}{\gamma_{\varphi\prime}}\right)} \tag{3}$$

$$N_c = (N_q - 1)\cot\left(\frac{\varphi'}{\gamma_{\varphi\prime}}\right) \tag{4}$$

$$N_\gamma = 2(N_q - 1)\tan\left(\frac{\varphi'}{\gamma_{\varphi\prime}}\right) \tag{5}$$

$\gamma_{c'}$, $\gamma_{\varphi'}$, and γ_γ are partial material factors equal to 1 (in the combination *A1 + M1 + R2*).

The weight of the load transfer platform is typically neglected for a relatively thin platform, and the superficial (third) term in equation (2) is omitted.

When a purely granular material is used as constitutive material of the load transfer platform, there is no cohesion, and the related term becomes null. Hence, equation (2) becomes:

$$q_p{}^+ = s_q N_q q_s{}^+ \tag{6}$$

For axisymmetric or plane-strain conditions, $s_q = 1$, and a relationship between q_p^+ and q_s^+, only function of φ', is established:

$$q_p{}^+ = N_q q_s{}^+ \tag{7}$$

A second equation is still necessary in order to determine the values of q_p^+ and q_s^+. This is performed using the load conservation equation:

$$\alpha q_p{}^+ + (1 - \alpha) q_s{}^+ = q_o \tag{8}$$

where α is the replacement ratio:

$$\alpha = \frac{A_c}{A_c + A_s} \tag{9}$$

where A_c is the area of inclusion and A_s the area of soil.

From equations (7) and (8), q_p^+ and q_s^+ can be expressed as a function of φ', α and q_0:

$$q_p{}^+ = \frac{N_q}{1 + \alpha\left(N_q - 1\right)} q_o \tag{10}$$

$$q_s{}^+ = \frac{1}{1+\alpha\left(N_q-1\right)} q_o \tag{11}$$

Within the framework of the ASIRI project (IREX, 2012), further research on Prandtl's failure mechanism has been carried out by centrifugal testing with various LTP thicknesses, rigid inclusion spacing and replacement ratios (Okyay, 2010). In Fig. 8, centrifuge test results are compared with limiting pressures calculated from Prandtl's theory, and it can be observed that a very good agreement exists between measured and theoretical values.

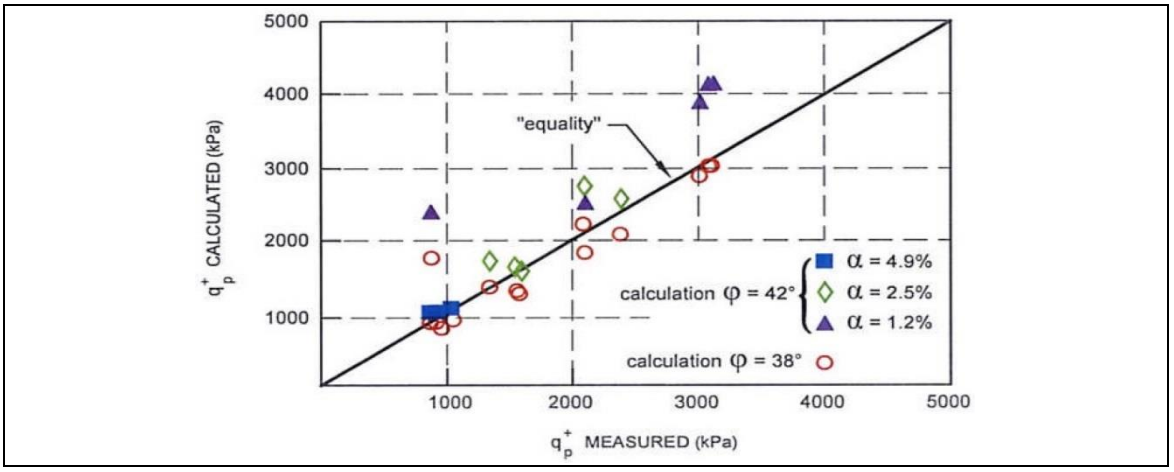

Figure 8: Comparison of measured limiting pressures (from centrifugal testing) with theoretical values calculated from Prandtl's theory (from IREX, 2012)

Within the framework of the ASIRI project (IREX, 2012), Prandtl's approach was also investigated by performing finite element calculations for various uniformly distributed loads. Figure 9 illustrates the results of this study. Figure 9 shows the pressures acting on the soil and on the inclusion head respectively on the abscissa and ordinate. The blue curve is obtained using equation (7). The slanted black lines correspond to the load conservation equation (8). The pink line is derived from finite element calculations. The stresses acting on the soil and on the inclusion and the value that can be mobilised at the head of the inclusion are also showed in Fig. 9. During the investigation, the Young modulus of the compressive soil was reduced for each uniform loading until the load transfer platform failed. It was observed that, at the last step prior to the failure, the stress at the inclusion head approached Prandtl's limit, but did not intersect it. Prandtl's failure mechanism can also be visualised by the distribution of the plastic points that are shown as red dots in Fig. 9.

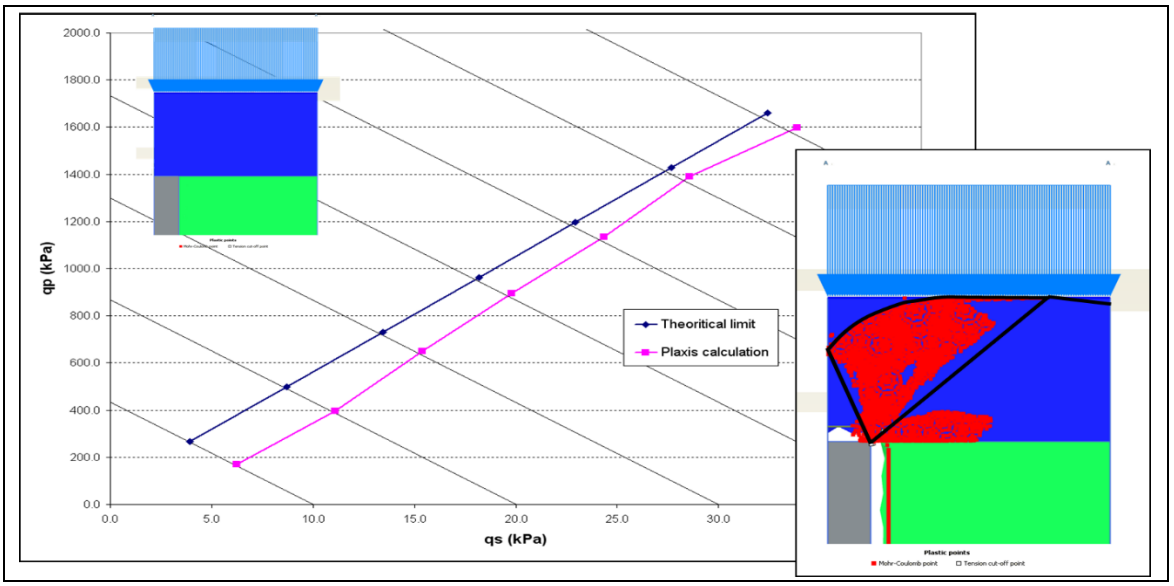

Figure 9: Comparison of limiting pressures calculated from finite element analyses and according to the Prandtl's theory (from IREX, 2012)

2.2.1.2. Punching shear failure mechanism

As illustrated in Fig. 7(b), the second failure mechanism can be modelled by envisaging a vertical shear cone within the granular layer of the load transfer platform. This failure mechanism only exists for thin load transfer platforms that are not covered by rigid structural elements, and is associated with the peak friction angle of the material.

According to Eurocode 7 - Design Approach 2 and from the shear cone geometry, the limit stress at the inclusion head is determined by using the applied external load, q_o, and the properties of the load transfer platform. Two configurations have to be considered as functions of the geometry of the inclusions and the load transfer platform, as illustrated in Fig. 10.

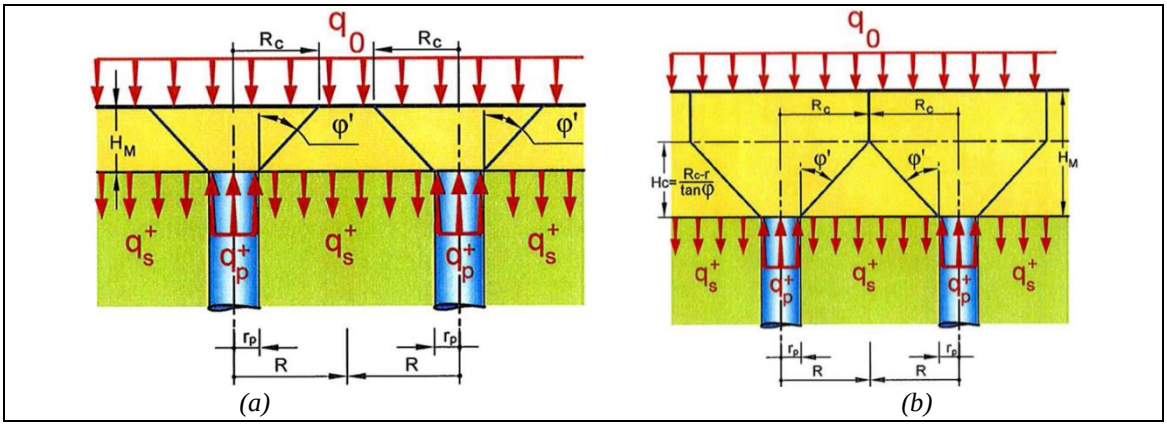

Figure 10: (a) Non-overlapping failure cones and (b) Overlapping failure cones (IREX, 2012)

In the first configuration, as shown in Fig. 10(a), the shear cones, developing above the inclusions, do not overlap. This condition is encountered when $H_M < H_c$, where H_c is defined as:

$$H_c = \frac{R - r_p}{\tan \varphi'} \tag{12}$$

where R is defined as:

$$R = \frac{s}{\sqrt{\pi}} \tag{13}$$

If the shear cones do not overlap (i.e. when $H_M < H_c$), $q_p{}^+$ is the weight of the cone plus the external load applied on the top circular side of the cone:

$$q_p{}^+ = \frac{H_M}{3}\left(\frac{R_c{}^2}{r_p{}^2} + 1 + \frac{R_c}{r_p}\right)\frac{\gamma}{\gamma_\gamma} + \frac{R_c{}^2}{r_p{}^2} q_0 + \frac{1}{\tan \varphi'}\left(\frac{R_c{}^2}{r_p{}^2} - 1\right)\frac{c'}{\gamma_{c'}} \tag{14}$$

where

$$R_c = r_p + H_M \tan\left(\frac{\varphi'}{\gamma_{\varphi'}}\right) \tag{15}$$

$\gamma_{c'}$, $\gamma_{\varphi'}$ and γ_γ are the partial material factors equal to 1 (in the combination *A1 + M1 + R2*).

In the second configuration, as shown in Fig. 10(b), the shear cones, developing above the inclusions, overlap. This condition is encountered when $H_M > H_c$. If the shear cones overlap, $q_p{}^+$ is the weight of the cone, the weight of the soil cylinder above it and the external load multiplied by the unit cell area:

$$q_p{}^+ = \left[\frac{H_c}{3}\left(\frac{R^2}{r_p{}^2} + 1 + \frac{R}{r_p}\right) + (H_M - H_c)\frac{R^2}{r_p{}^2}\right]\frac{\gamma}{\gamma_\gamma} + \frac{R^2}{r_p{}^2} q_o + \left[\frac{1}{\tan \varphi'}\left(\frac{R^2}{r_p{}^2} - 1\right)\right]\frac{c'}{\gamma_{c'}} \tag{16}$$

with $\gamma_{c'}$ and γ_γ are equal to 1.

2.2.2. Ultimate Limit State (ULS) stress domain of the concept

In order to fully understand the concept of rigid inclusions with a load transfer platform, the domain of admissible stresses at the base of the load transfer platform has to be considered prudently.

Figure 11 graphically presents the ULS stress domain at the base of the load transfer platform.

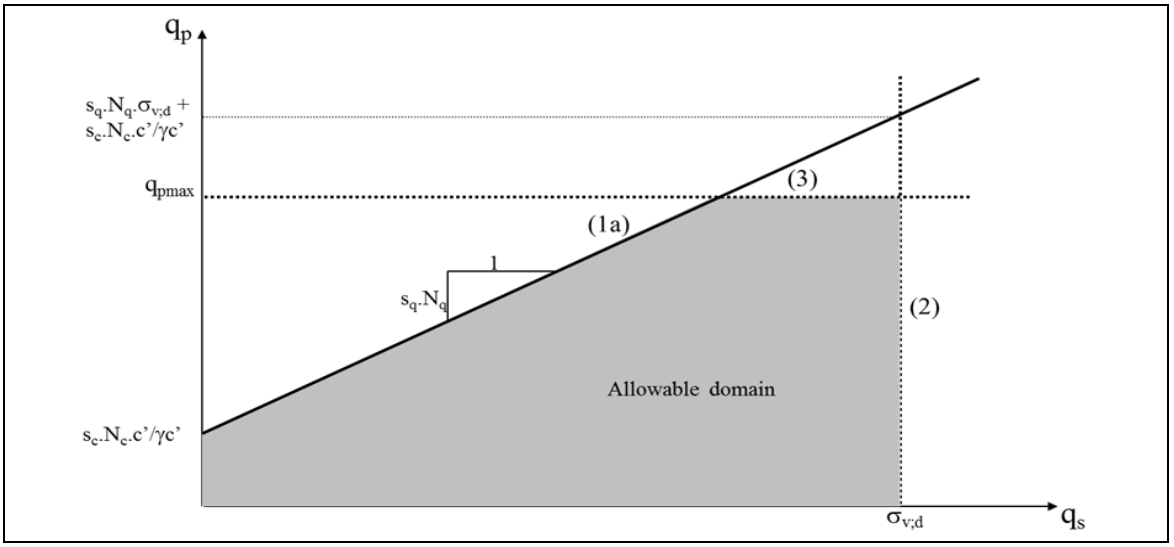

Figure 11: Domain of admissible stresses (ULS) at the base of the load transfer platform (IREX, 2012)

When failure occurs by Prandtl's mechanism, regardless of the load level, the stress domain in the load transfer platform is firstly limited by the Prandtl line according to equation (2) or more generally according to equation (7) represented by line (1a) in the figure.

The stress on the *in-situ* soil, q_s^+, is limited, at ULS, by the allowable stress $\sigma_{v;d}$, which is determined on the basis of the soil study; for example with the appropriate partial factors applied on P_{LM}, the limit pressure of the Ménard pressuremeter test:

$$\sigma_{v;d} = \frac{k_p P_{LM}}{\gamma_{R;v} \cdot \gamma_{R,d}} \tag{17}$$

where $\gamma_{R;v}$ is the partial resistance factor for spread foundations (equal to 1.4 according to Table A.5 of Eurocode 7), and $\gamma_{R;d}$ is the appropriate model factor.

This allowable stress, $\sigma_{v;d}$, limits the domain with line (2) of Fig. 11.

q_p^+ is limited by the load bearing capacity of the inclusion (according to the philosophy of Eurocode 7) and by the maximum allowable stress for the constitutive material of the rigid inclusion (according to the philosophy of Eurocode 2):

$$q_p^+ < q_{p,max} < min\left(\frac{{}^{R_b}/_{\gamma_b \cdot \gamma_{R,d}} + {}^{R_s}/_{\gamma_s \cdot \gamma_{R,d}}}{\pi {r_p}^2}; f_{c,d}\right) \tag{18}$$

where γ_b and γ_s are the partial factors respectively for the base (R_b) and the shaft (R_s) resistances. The assessment of the base and shaft resistances and the calculation of the design value $f_{c,d}$ will be the subjects of the following paragraphs. As observed in Fig. 11, $q_{p,max}$ limits the domain with line (3).

When the load transfer platform is thin and not covered by a rigid structural element (such as a slab on grade, a raft or footings), the stress domain has to be partially limited. This is illustrated in Fig. 12 where the load transfer platform is thin, not covered by rigid structural elements and the failure cones do not overlap. Here, the stress domain is limited by the dashed blue line (1b), which corresponds to equation (14). If the failure cones overlap, a second curve is added to limit the stress domain, as illustrated in Fig. 13, with the dashed red curve corresponding to equation (16).

Finally, in order to satisfy the load conservation equation (8), q_s^+ and q_p^+ have to be on the diagonal blue line that is shown in Fig. 14. For a given load q, the admissible domain will reduce to this segment. The calculated design value $q_{p,d}^+$ is therefore calculated by solving Prandtl's equation (7) and the load conservation equation (8) simultaneously. That situation corresponds to the red square in Fig. 14.

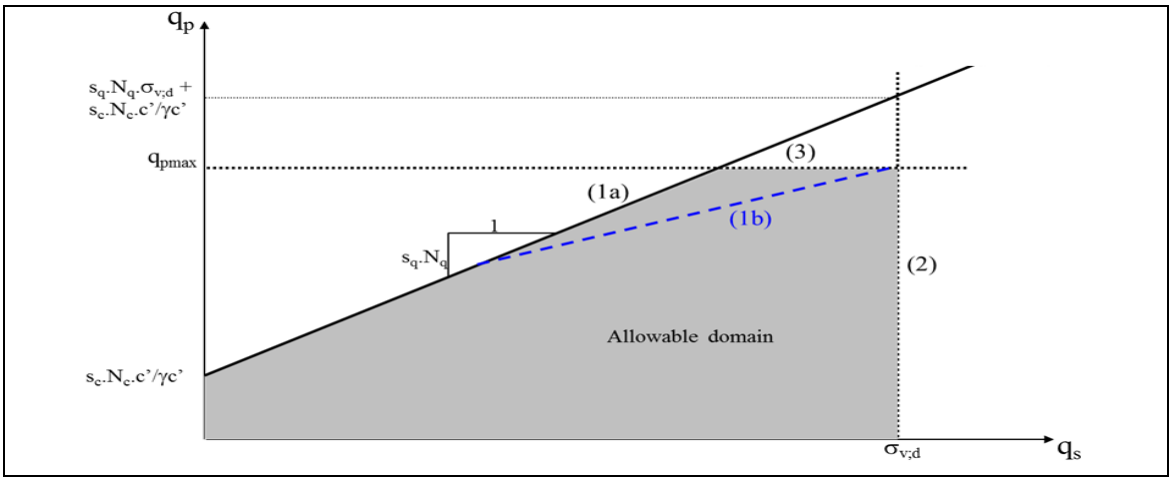

Figure 12: Domain of admissible stresses (ULS) at the base of the load transfer platform when the load transfer platform is thin, not covered by rigid structural element and the failure cones do not overlap (IREX, 2012)

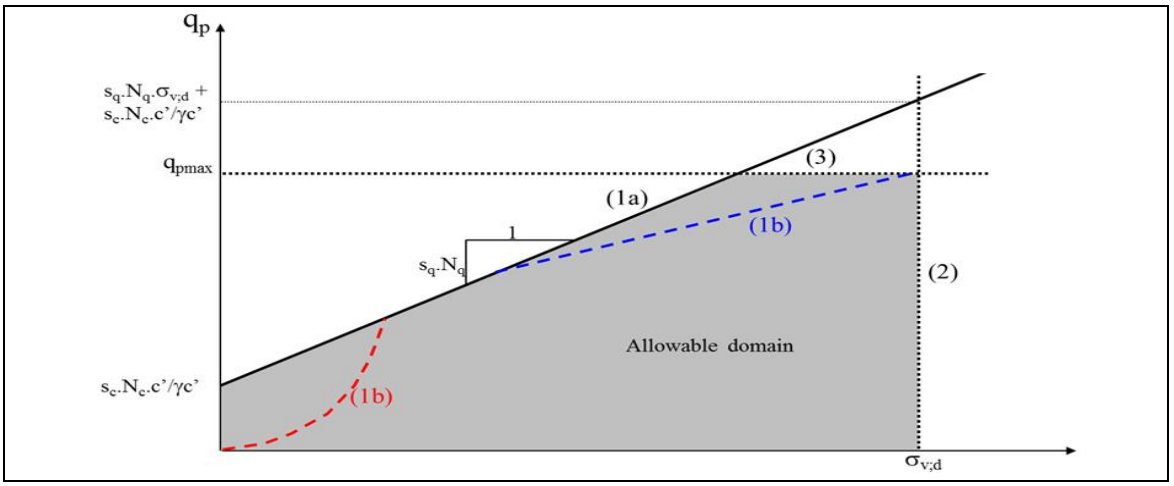

Figure 13: Domain of admissible stresses (ULS) at the base of the load transfer platform when the load transfer platform is thin, not covered by rigid structural element and the failure cones overlap (IREX, 2012)

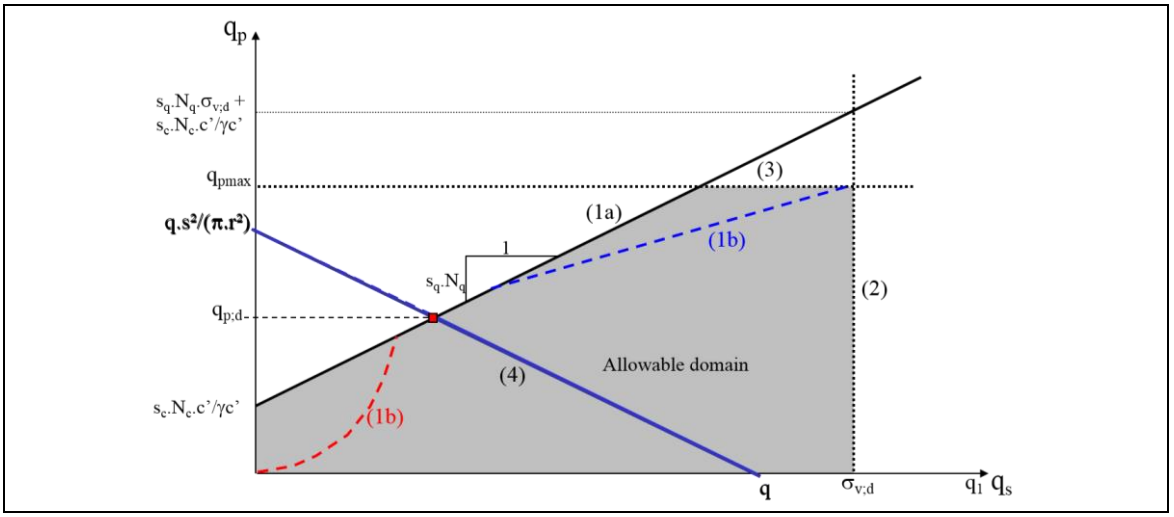

Figure 14: Domain of admissible stresses (ULS) at the base of the load transfer platform with consideration of the load conservation equation (IREX, 2012)

As a consequence, $q_{p,d}^+$ is a function of

- the load q,
- the diameter of the rigid inclusions,
- the inclusion grid size,
- the thickness of the load transfer platform,
- the parameters of the load transfer platform (c', φ' and γ).

$q_{p,d}^+$ is thus independent of the deformability of the various underlying soil layers.

Nevertheless, while $q_{p,d}^+$ is the intersection of Prandtl's equation (7) and the load conservation equation (8), the pair (q_p^+; q_s^+), which is actually mobilized, can be anywhere on this diagonal segment (line 4 in Fig. 14), and its actual position will depend on the compressibility of the various soil layers directly below the load transfer platform. If the soil is very soft, then the mobilized pair will be close to the limit design value $q_{p,d}^+$, but if the soil is quite dense, then the pair will be away from this limit design value.

It is important to note that, as shown in Fig. 15, changes of the external load moves the equilibrium in the plane (q_p^+; q_s^+) along a curve that tends towards an asymptote for large loads; i.e. an increase in loading also increases the efficiency towards its maximum value, but is never able to create internal failure of the load transfer platform by intersecting Prandtl's equation (7).

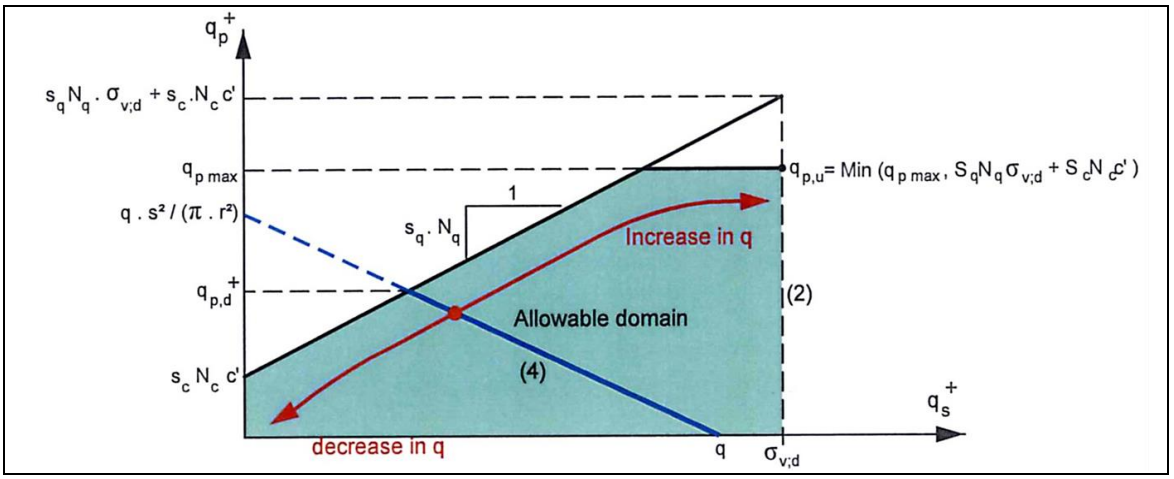

Figure 15: $q_{p,d}^+$ and deformability of various soil layers (IREX, 2012)

2.2.3. Geotechnical limit states (GEO) – consideration of the negative skin friction

It must be verified that the forces, mobilized at the base and throughout the rigid inclusion, do not exceed the limit values computed in agreement with Eurocode 7. The base and the shaft resistances of the rigid inclusion will be determined using the results of the geotechnical investigation (such as cone penetrometer tests or Ménard pressuremeter tests). In Belgium, this is realized considering the guidelines of the Rapport 12 of the Belgian Building Research Institute (BBRI) published in 2009, and which are currently under revision. In France, the standard NF P 94-262 has to be applied.

If the behavior at the base of the rigid inclusion is commonly regarded to be in accordance with the principles of Eurocode 7, special attention has to be given to the shaft behavior. Indeed, as previously mentioned in this keynote, a differential settlement arises between the soft soil and the heads of the rigid inclusions at the base of the load transfer platform. This differential settlement creates a negative skin friction along the rigid inclusions at shallow depth. The consideration of this negative skin friction is therefore relevant for the geotechnical design of the rigid inclusion.

After the verification of the positive fiction arising below depth h_c, according to Eurocode 7 and its various national annexes, the negative skin friction which develops above depth of h_c has to be assessed. As reported in IREX (2012), it must be verified that the friction τ of the soil along the inclusion shaft (above the depth h_c) does not exceed the following limit value:

$$\tau < \sigma_v' \, K \tan \delta \tag{19}$$

where σ_v' is the vertical stress calculated along the inclusion. K tanδ is an empirical parameter, which is given in Combarieu (1985) or more recently in the French standard NF P 94-262.

Within the framework of the ASIRI project (IREX, 2012), an advanced methodology is also provided allowing the assessment of the negative skin friction and the determination of the critical height, h_c.

2.2.4. Structural limit states (STR) of the rigid inclusion – definition of $f_{c,d}$

In order to design the rigid inclusion, its compressive strength for axial loading (usually denoted by UCS for Uniaxial Compressive Strength) has to be defined. In the philosophy of the Eurocodes, a design value of the uniaxial compressive strength of the material, noted $f_{c,d}$, is then computed.

2.2.4.1. $f_{c,d}$ for a classical concrete pile – according to Eurocode 2

For a classical concrete pile, the designer could refer to the content of Eurocode 2 where $f_{c,d}$ is defined as:

$$f_{c,d} = \frac{\alpha_{cc} f_{c,k}}{\gamma_c} \tag{20}$$

where γ_c is the partial safety factor for concrete, α_{cc} is the coefficient taking account of long term effects on the compressive strength and of unfavourable effects resulting from the way the load is applied and $f_{c,k}$ is the characteristic (5%) cylinder compressive strength of the concrete material determined in accordance with European standard EN 206-1. The characteristic strengths for $f_{c,k}$ and the corresponding mechanical characteristics necessary for design of concrete material, are given in Table 3.1 of Eurocode 2. It is to note that, in agreement with Eurocode 2, the partial factor for concrete γ_c should be multiplied by a factor, k_f, for calculation of design resistance of cast in place piles without permanent casing.

2.2.4.2. $f_{c,d}$ for a rigid inclusion - according to the ASIRI project (IREX, 2012)

Within the framework of the ASIRI project (IREX, 2012), a methodology is proposed for the calculation of the design and characteristic values of the UCS of the material for the rigid inclusions:

$$f_{c,d} = min\left(\alpha_{cc} k_3 \frac{f^*_{c,k}}{\gamma_c}; \alpha_{cc} \frac{f_{c,k}(t)}{\gamma_c}; \alpha_{cc} \frac{C_{max}}{\gamma_c}\right) \tag{21}$$

where α_{cc} is a coefficient depending on the presence or absence of steel reinforcement (reinforced = 1, non-reinforced = 0.8). γ_c is a partial coefficient with a value equal to 1.5 at the fundamental ULS and 1.2 at the accidental ULS. $f_{c,k}$* is the characteristic value of the compressive strength of the concrete, grout or mortar in the inclusion, as determined in the following formula:

$$f^*_{c,k} = min\left(f_{c,k}(t); C_{max}; f_{c,k}\right) \frac{1}{k_1 k_2} \tag{22}$$

where $f_{c,k}$ is the characteristic value of the compressive strength measured on cylinders at 28 days of hardening, $f_{c,k}(t)$ is the characteristic value of the compressive strength measured on cylinders at time *t* and C_{max} is the maximum compressive strength value taking into account the required consistency of the fresh concrete, grout or mortar, depending on the technique used, as shown in Table 2.

Table 2. Assigned values of C_{max} and the coefficient k_1 (from IREX, 2012)

Case	Execution mode	C_{max} (MPa)	k_1
1	Drilled inclusions with soil extraction	35	1.3
2	Drilled inclusions using a hollow auger with soil extraction	30	1.4
3	Drilled inclusions using a hollow auger with soil displacement	35	1.3
4	Inclusions either vibratory driven or cast in place	35	1.3
5	Incorporation of a binder with the soil (treated soil-columns, jet grouting…)	(*)	(**)

(*) Value to be determined through field testing

(**) Columns of treated soil using a mechanical tool that guarantees the cross-section geometry: k_1 to be determined on a case-by-case basis with $k_1 > 1.3$

k_1 is a value depending on both the drilling method and slenderness ratio, as listed in Table 2. According to IREX (2012), for a soil treated by jet grouting or with a tool that does not guarantee a homogeneous section geometry, the value of k_1 has to be determined on a case-by-case basis $k_1 > 1.5$. k_1 may be decreased by 0.1, only for drilled inclusions when the composition of the ground layers guarantees stability of the outer borehole walls or when the inclusion is cased and concreted in the dry (a guarantee of borehole wall stability must be demonstrated using the procedure outlined in the EN 1536 bored pile execution Standard).

k_2 depends on the slenderness ratio:
k_2 = 1.05 for inclusions whose ratio of smallest dimension *d* to length is less than 1/20;
k_2 = 1.3-d/2 for inclusions whose smallest dimension is less than 0.60 m;
k_2 = 1.35-d/2 for inclusions combining the two previous conditions.

k_3 depends on the type of control performed on the rigid inclusions (see IREX-2012 for more information).

2.2.4.3. $f_{c,d}$ for soil mix elements - according to the BBRI Soil Mix project (2009-2013)

If the computation of the design value, according to the ASIRI project (IREX, 2012), is not too complex for a rigid inclusion executed with a classical method (drilled inclusions with or without soil extraction), the computation of $f_{c,d}$ for a jet grout column or a soil mix element is no easy task according to this approach. Within the framework of the BBRI soil mix project (2009-2013), a methodology has been developed to compute the design and characteristic UCS values for soil mix material based on a simplified approach.

In the BBRI approach, the characteristic UCS value of the soil mix material can be computed with the help of two different methods depending on the number of test samples defined in agreement with the quality control requirements of the project (see the SBRCURnet/BBRI soil mix handbook, 2016).

The first approach allows the computation of the characteristic UCS value on the basis of a statistical analysis. As the theoretical statistical distribution is not always easy to identify (e.g. in the presence of sub-populations in the histogram of the test results), the UCS characteristic value is computed as the 5% quantile of the cumulative curve of the results of the UCS tests performed at 28 days of hardening on *in-situ* core samples. This approach is only possible if the number of test samples is larger than 20. Otherwise, a second methodology, which is based on the German standard DIN 4093 (2012), will be used.

In this second approach, which is valid when the number of test samples is less than 20, the UCS characteristic value will be computed as the minimum of three values:

- the minimal value of all the test results,
- the arithmetic average value of all the test results multiplied by a constant reduction factor α equal to 0.7.
- a maximum value of 12 MPa.

The constant reduction factor α was determined on the basis of the results of large-scale UCS tests performed on real-scale soil mix elements and represents the scale effect as discussed in Denies et al. (2013 and 2014).

In order to consider the heterogeneous character of the soil mix material and the representativity of the classical test samples (typically 10 cm diameter and 20 cm high), an elimination rule is introduced in the computational process. For a particular construction site, all samples are tested, then based on the observations of the test operator, an elimination process is applied according to Ganne et al. (2010) who have proposed to reject all test samples with unmixed soft soil inclusions that are larger than 1/6 of the sample diameter, on condition that no more than 15% of the test samples from one particular site would be rejected. The possibility to reject test samples results from the notion that an unmixed soft soil inclusion that is 20 mm or smaller does not influence the behavior of a soil mix structure. On the other hand, an unmixed soft soil inclusion of 20 mm in a test sample of 100 mm diameter significantly influences the test result. Of course, this condition is only suitable if one assumes that there is no unmixed soft soil inclusion larger than 1/6 of the width of the *in-situ* soil mix structure.

Figure 16 summarizes the BBRI methodology to compute the characteristic UCS value of the soil mix material.

As soon as the UCS characteristic value of the soil mix material at 28 days is determined, the design value $f_{c,d}$ can be computed:

$$f_{c,d} = \alpha_{sm} \frac{f_{c,k}}{\gamma_{SM}\, k_f} \beta \tag{23}$$

where:

- α_{sm} is a coefficient that takes the long term effects on the compressive strength and of unfavourable effects resulting from the way the load is applied (only applied if the lifetime of the soil mix elements is larger than 2 years) into account. For temporary situations (lifetime < 2 years), α_{sm} is equal to 1 and for permanent situations (lifetime > 2 years), α_{sm} is equal to 0.85 according to the SBRCURnet/BBRI soil mix handbook (2016).

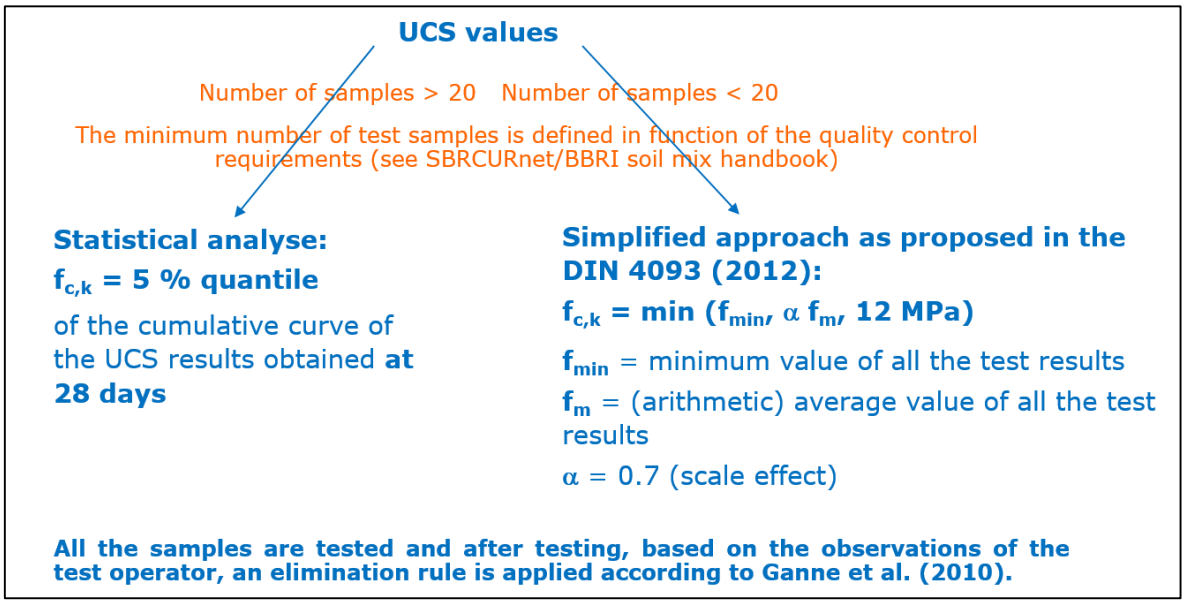

Figure 16: BBRI methodology to compute the characteristic UCS value of the soil mix material

- γ_{SM} is a partial material factor.
- The factor k_f, previously mentioned for concrete piles, is defined in the paragraph 2.4.2.5 (2) of Eurocode 2. k_f is considered in order to differentiate the hardening conditions (in laboratory or *in-situ*). If the UCS is determined on samples directly cored in the hardened soil mix elements previously installed *in-situ*, k_f is equal to 1; otherwise k_f is equal to 1.1.
- β is a correction factor that takes the age of the soil mix material into account (consult SBRCURnet/BBRI soil mix handbook 2016 for more information); β is equal to 1 at 28 days of hardening.

Table 3 summarizes the values used for the different partial factors as used in Belgium and in The Netherlands according to the guidelines of SBRCURnet/BBRI soil mix handbook (2016).

Table 3: Factors for the computation of the UCS design value, $f_{c,d}$, of the soil mix material (SBRCURnet/BBRI soil mix handbook – 2016)

	Factors for the computation of the design value $f_{c,d}$ of the soil mix material (Belgium – The Netherlands)			
	γ_{SM} (Persistent-transient/ accidental)	α_{sm} (temporary/ permanent)	k_f (UCS based on experience/ UCS tests on *in-situ* core samples)	β
ULS DA1-1 (Belgium) ULS DA3 (The Netherlands)	1.50/1.20	1.00/0.85	1.10/1.00	Depending on the age of the material – see SBRCURnet/BBRI soil mix handbook (2016) β = 1 at 28 hardening days

2.2.4.4. $f_{c,d}$ for jet grout columns - according to the German standard DIN 4093 (2012)

It can be noted that German Standard DIN 4093 (2012) also proposes a methodology to compute a characteristic value for the soil mix and the jet grouting material. This methodology is similar to the simplified approach, as presented in Fig. 16, but with a variable value of α (computed with an iterative process) and with a maximum value of 10 MPa for the jet grout material. This methodology was notably discussed in Topolnicki and Pandrea (2012) and in Denies et al. (2013).

It can be noted that all these computational methodologies (ASIRI project, BBRI soil mix project and DIN 4093) are in line with the philosophy of Eurocodes using partial safety factors.

2.2.5. Edge behavior of the load transfer platform

Stress distribution at the edge of the loading zone, where Prandtl's failure mechanism does not fully develop is somewhat different. The horizontal length of development of the Prandtl curve, denoted L_{max}, is computed as:

$$L_{max} = \frac{\cos\left(\pi/4 - \varphi'/2\right)}{\cos\left(\pi/4 + \varphi'/2\right)} D.\, e^{-\tan(\varphi').\pi/2} \quad (24)$$

As shown in Figure 17(a), Prandtl's mechanism can fully develop in the load transfer platform if the overhang length of the footing, denoted L, is greater than L_{max}. The limit pressure at the inclusion head q_p^+ is then computed as described in the Section 2.2.2 according to the Prandtl mechanism (equation 7).

In the case shown in Figure 17(b), the edge of the inclusion corresponds to the edge of the footing. The overhang is then zero and the load applied to the footing is nearly fully transmitted on the inclusion head. The vertical stress on the peripheral soil, which is due to the surrounding ground, is equal to γH. Considering the decomposition of the engineering issue into an active limit state equilibrium and a passive limit state equilibrium, as illustrated in Fig. 18, it is possible to obtain the two following equations describing the role of the stress q in Volume 1 (active earth pressure) and Volume 2 (passive earth pressure):

$$q = q_p^+ K_{q1} \quad (25)$$

$$q = \gamma H K_{q2} \quad (26)$$

where $K_{q,1}$ and $K_{q,2}$ can be estimated considering the Caquot and Kerisel theory (1966), which is valid for a weightless medium. Considering equations (25) and (26), it is possible to write $q_p^+/\gamma H = K_{q,2}/K_{q,1} = N_q^*$, which is a bearing factor depending on the friction angles of the material of the load transfer platform (φ_1) and of the surrounding soil (φ_2). The N_q^* values that are computed within the framework of the ASIRI project (IREX, 2012) considering the Caquot and Kerisel theory (1966) are shown in Table 4.

Table 4: N_q^* values based on load transfer platform (LTP) and surrounding soil friction angles

LTP φ_1	**N_q^* (φ_1)**	**Soil φ_2= 15°**	**Soil φ_2= 20°**	**Soil φ_2= 25°**	**Soil φ_2= 30°**
		N_q^*	**N_q^***	**N_q^***	**N_q^***
30	18.4	6.98	9.45	13.08	18.43
33	26.1	7.86	10.64	14.71	20.88
35	33.3	8.52	11.53	16.01	22.67
38	48.9	9.68	13.05	18.11	25.80
40	64.2	10.54	14.29	19.71	28.04

As shown in Fig. 17(c), when the footing overhang is between 0 and L_{max}, the limiting pressure at the inclusion head can be estimated using a linear interpolation between these two extreme values. This is shown in Fig. 19.

Generally, when more than one inclusion is installed beneath the footing, the edge effect that has been described is applicable to only a fraction of the inclusion depending on whether the inclusion is at the footing corner or side. As illustrated in Fig. 20, the edge limit stress, $q_p^+(L)$, is applicable only to the exterior portion of the perimeter, the limit stress calculated from Prandtl's failure mechanism, $q_p^+(P)$, applies to the inner portion of the inclusion, and the resulting value must be a weighted average of these two terms.

By analogy with the distribution of negative friction within a group of piles, IREX (2012) proposes that limit stress values on the inclusion heads under the footing be determined using the weighting relationships shown in equations (27) to (31).

For single row inclusions that are shown in Figure 21(a):

$$q_{p,a}{}^+ = \frac{1}{3} q_p{}^+(P) + \frac{2}{3} q_p{}^+(L) \quad (27)$$

$$q_{p,e}{}^+ = \frac{2}{3} q_p{}^+(P) + \frac{1}{3} q_p{}^+(L) \quad (28)$$

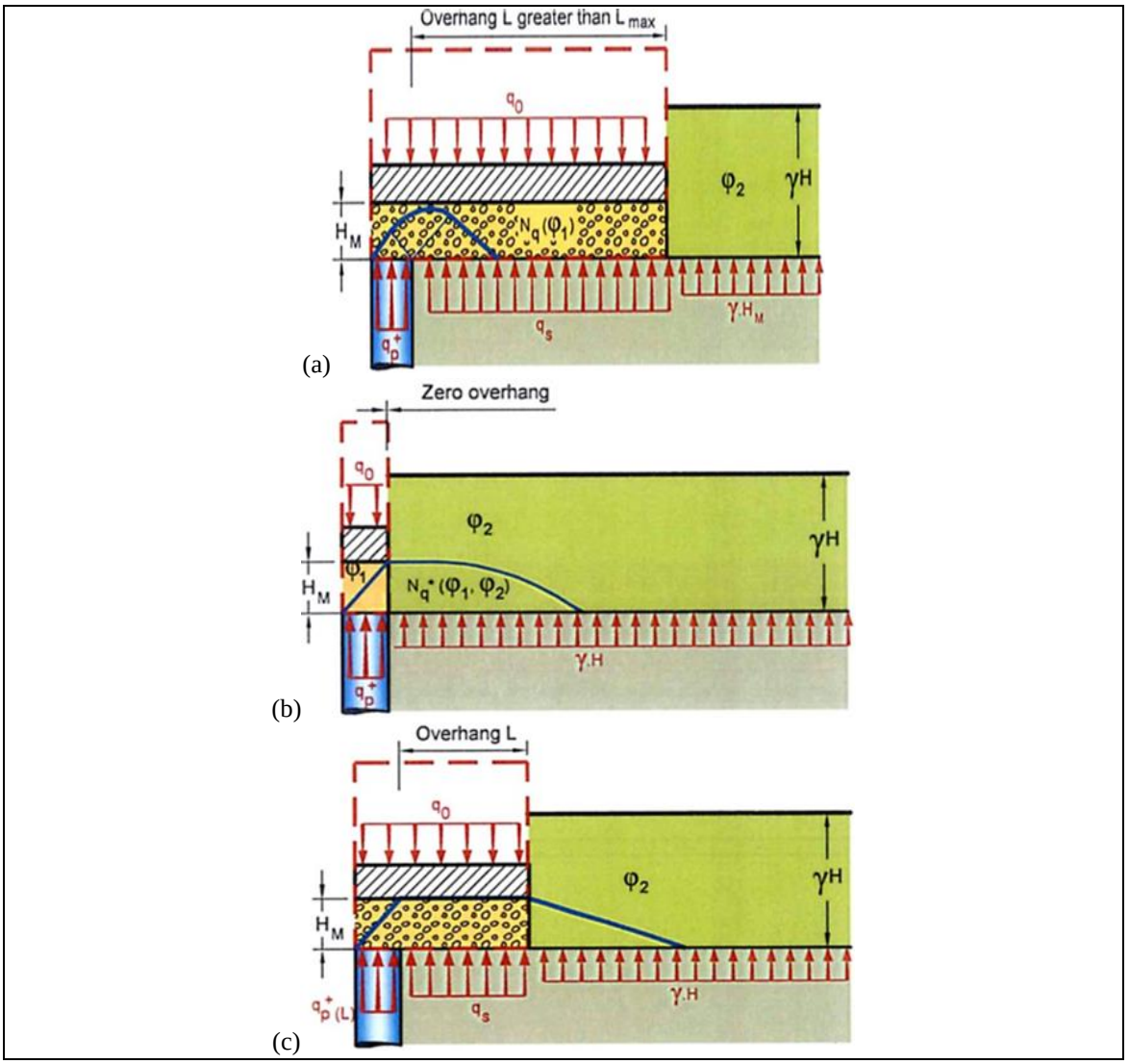

Figure 17: Configurations considered for the study of the edge behavior (IREX, 2012)

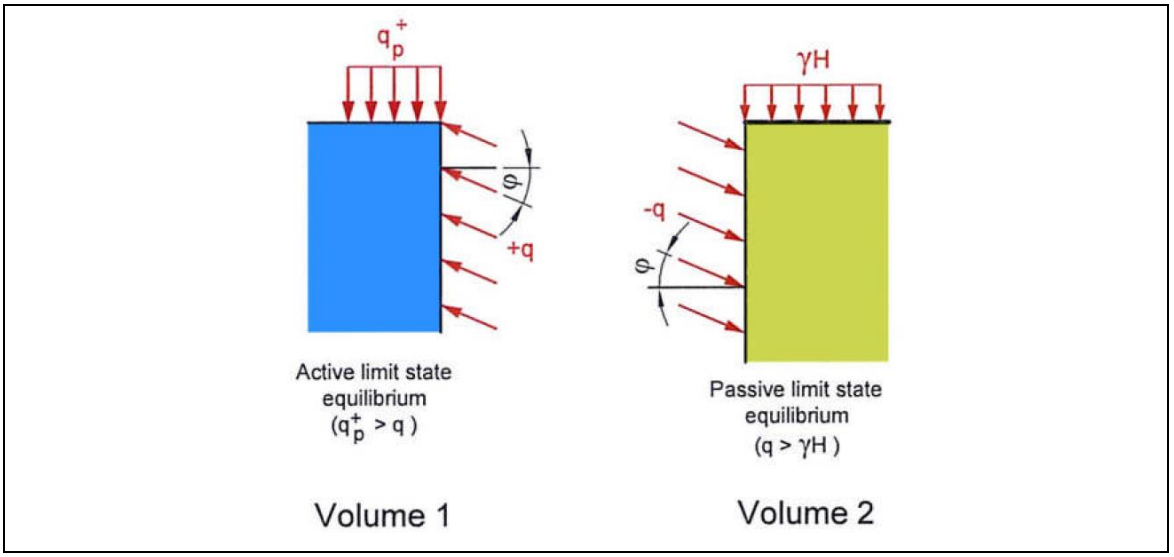

Figure 18: Decomposition into an active limit state equilibrium and a passive limit state equilibrium (IREX, 2012)

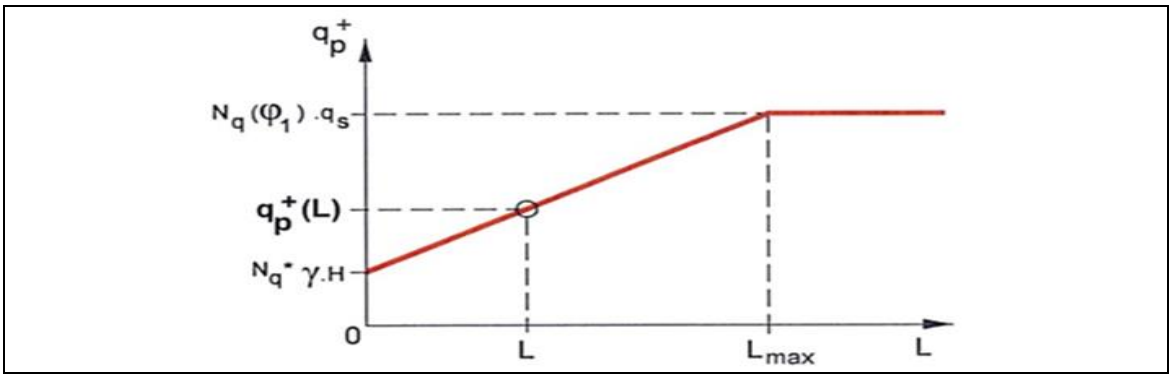

Figure 19: Principle used to determine the threshold stress on the inclusion head by interpolating between the extreme values for an overhang greater than L_{max} and a zero overhang (IREX, 2012)

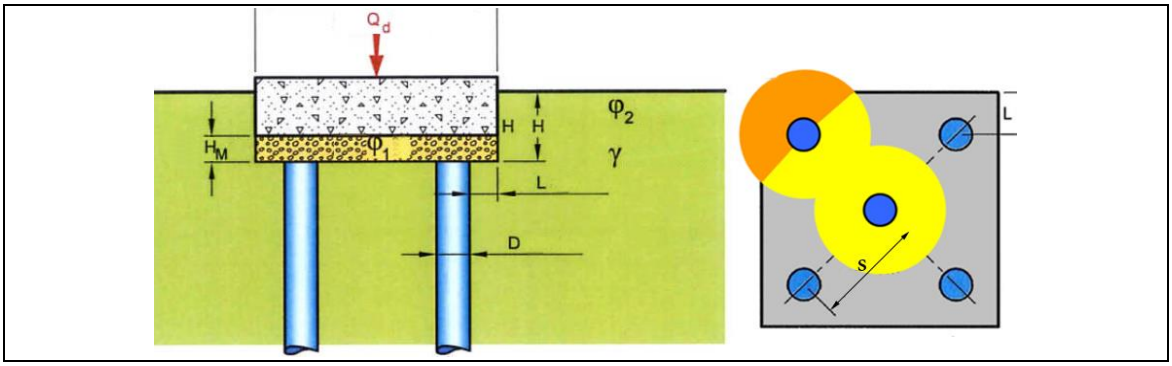

Figure 20: Edge effect combination, modified from ASIRI (IREX, 2012)

For multiple rows of inclusions that are shown in Figure 21(b):

$$q_{p,i}{}^{+} = q_p{}^{+}(P) \tag{29}$$

$$q_{p,a}{}^{+} = \frac{7}{12} q_p{}^{+}(P) + \frac{5}{12} q_p{}^{+}(L) \tag{30}$$

$$q_{p,e}{}^{+} = \frac{5}{6} q_p{}^{+}(P) + \frac{1}{6} q_p{}^{+}(L) \tag{31}$$

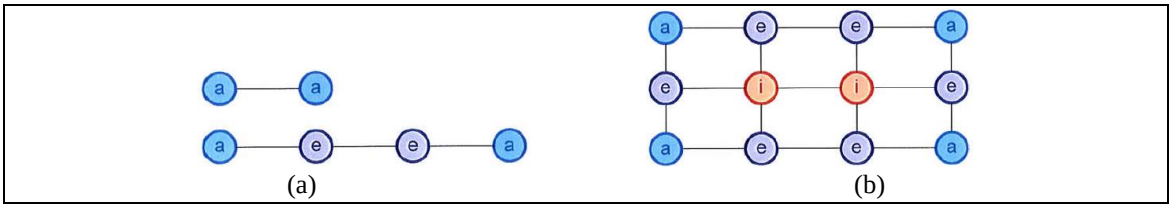

Figure 21: (a) Edge effect combination for single row of inclusions, and (b) Edge effect combination for multiple rows of inclusions (IREX, 2012)

2.2.6. Other design aspects

In the ASIRI publication (IREX, 2012), other design aspects, not discussed here, are well considered by the authors, such as:

- the SLS design approach and the topic of the settlements,
- the design of the foundation slabs installed above the load transfer platform,
- the design of potential geosynthetics installed in the granular load transfer platform,
- the transfer of the lateral loads to the rigid inclusions and the surrounding soil,
- the lateral and flexural behaviors of the rigid inclusions,
- the consideration of seismic loads,
- the soil investigation and testing,
- some execution and quality control (monitoring) aspects,
- etc.

2.3. Piled embankment – The Dutch approach (CUR-rapport 226)

In the present keynote, the authors mainly present the concept of rigid inclusions combined with a load transfer platform on the basis of the guidelines published by IREX (2012) as a result of the ASIRI research project. If there are other guidelines available worldwide focusing on this concept, few publications present a design methodology in line with the philosophy of the Eurocodes, which is a major point for European engineers. In order to offer, to the designers, geotechnical alternative solutions comparable with the classical piling solution, it is quite important to develop design guidelines for the ground improvement solutions respecting the concepts of the Eurocodes. The engineers have to compare the two geotechnical solutions (ground improvement and piling) on a similar basis governed by the principles of the Eurocodes.

The guidelines "Ontwerprichtlijn paalmatrassystemen" of the SBRCURnet (CUR rapport 226, 2010), in The Netherlands, falls into this category. This publication involves a guideline for the design of piled embankments with geosynthetic reinforcement generally at the base of the load transfer platform, such as illustrated in Fig. 22. A large amount of fundamental concepts described in these guidelines can be used for the design of rigid inclusions combined with a load transfer platform. Subsequent to a survey of the requirements and the basic principles for the structure as a whole, these guidelines give the design of the pile foundation, the design of the "mattress" (i.e. the load transfer platform) with the geosynthetic reinforcements, the execution and the maintenance.

The CUR-rapport 226 (2010) includes many practical design guidelines based on literature studies and on the results of 2D and 3D finite element calculations. The results of these numerical calculations have been compared with measurements from practical projects. Considering this comparison, primary directives of the German EBGEO guidelines, also written in agreement with the Eurocodes, have been adopted. Indeed, a special interest of the Dutch guidelines is the discussion of different design methodologies (EBGEO, BS 8006, etc.) and the application and comparison of these methods with practical case studies.

Even if the principles behind piled embankments sometimes differ from the concept of rigid inclusions combined with a load transfer platform, it can still constitute a source of inspiration for the geotechnical designers who are specialized in the design of rigid inclusions.

A particular aspect which is deeply investigated in the Dutch approach is the design of the geosynthetic reinforcements installed at the base of the load transfer platform. This design is performed considering the particular load transfer distribution that develops in the load transfer platform.

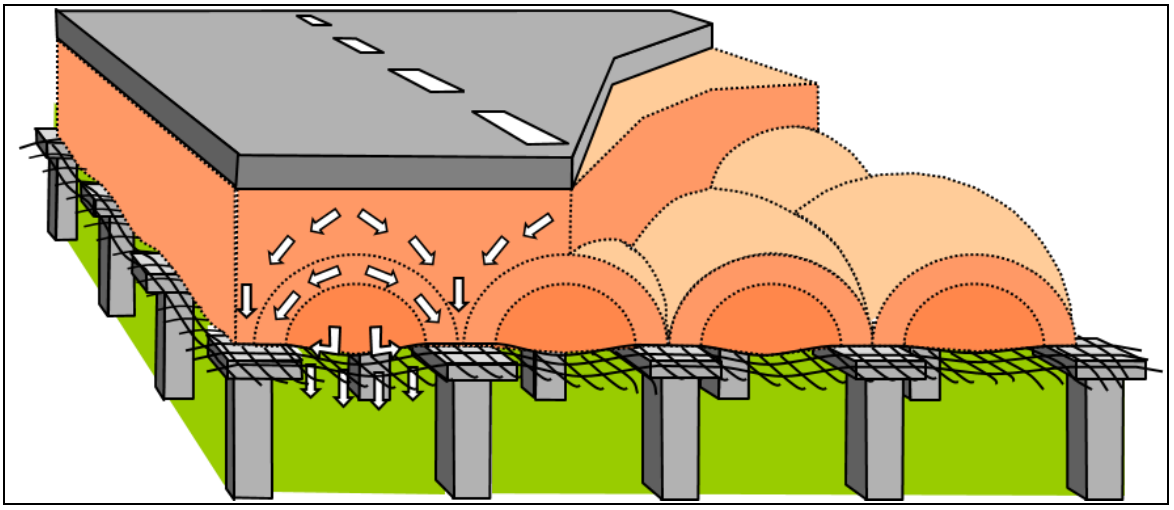

Figure 22: Concept of piled embankment as covered by the Dutch guidelines CUR-rapport 226 (2010)

2.4. Piled embankment - Study of the load transfer distribution

Since many years ago, Suzanne Van Eekelen (Deltares) has studied the nature of load distribution developing (through the load transfer platform) over the geosynthetic reinforcements and the rigid inclusions in piled embankments. Van Eekelen et al. (2013) have recently presented a new model, called concentric arches model, such as illustrated in Fig. 23, to improve the understanding of arching effect in the load transfer platform and to optimize the design of the concept. In this model, the load is transferred along the concentric 3D hemispheres towards the geosynthetic reinforcement strips and then via the concentric 2D arches towards the pile caps.

As reported in Van Eekelen and Bezuijen (2012), the geosynthetic reinforcement strains from the vertical load are usually calculated in two steps. In the first step, the vertical load is divided into two parts. As illustrated in Fig. 24, the first part, called "A", is directly transferred to the piles, and the remainder, is called "B+C'. Part "A" is relatively large due to arching. EBGEO and CUR-rapport 226 (2010) adopted Zaeske's model (Zaeske, 2001) for this calculation step. British standard BS8006 adopted Marston's model (1913), and modified it to acquire a 3D model (as described in Van Eekelen et al., 2011 and Lawson, 2012). In the second step, the vertical load is further divided into load "B" that is transferred through the geosynthetic reinforcement to the piles and the load "C" that is carried by the subsoil. Loads "A", "B" and "C" are all vertical loads.

As described in Van Eekelen and Bezuijen (2012), it is assumed that the strains mainly occur in the geosynthetic reinforcement strip. Assuming a load distribution on this strip, and the support from the subsoil (if permissible), the geosynthetic reinforcement strains can be calculated. CUR-rapport 226 (2010) and EBGEO approaches consider a triangular distribution of the load on the geosynthetic reinforcement strip, while British Standard BS8006 adopts an equally distributed load, and excludes subsoil support in the calculations. Nevertheless, based on experimental studies, Van Eekelen and Bezuijen (2012) have highlighted the fact that the distribution of the load on the reinforcement strip between two piles tends to have the distribution of an inverse triangle (see Fig. 25). To draw this conclusion, a series of nineteen piled embankment model experiments was carried out in the Deltares laboratory to understand why the predicted geosynthetic reinforcement strains were always larger than the measured *in-situ* geosynthetic reinforcement strains within the framework of actual construction sites.

As shown by the results of this experimental study, there are still research perspectives for the study of the rigid inclusion concept especially concerning the load transfer distribution developing in the load transfer platform.

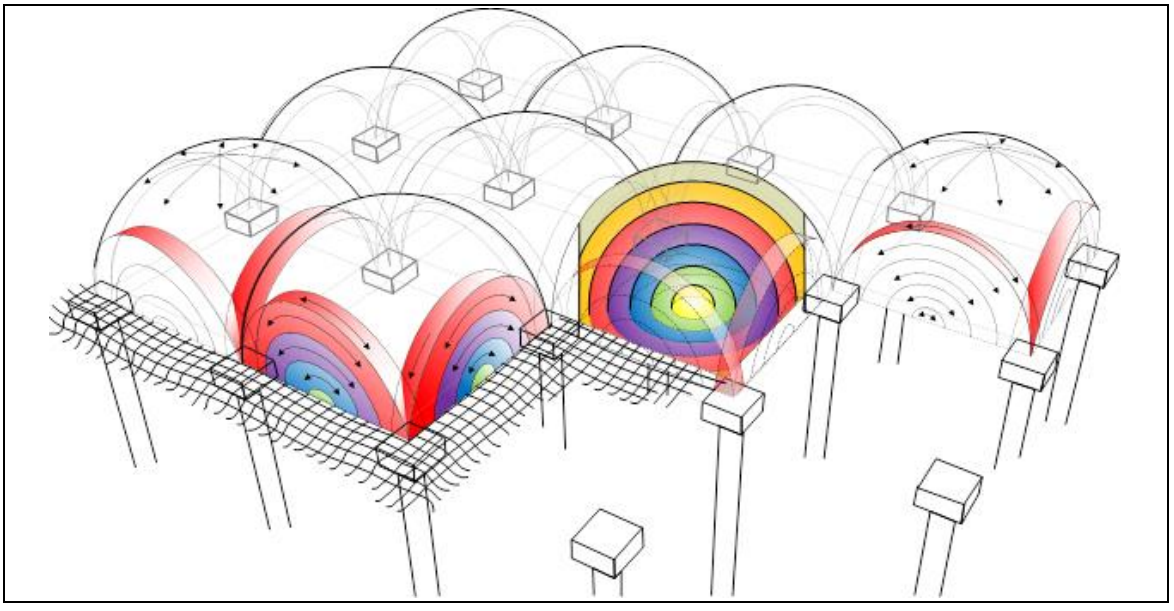

Figure 23: New design model (Concentric Arches model) developed by Van Eekelen et al. (2013)

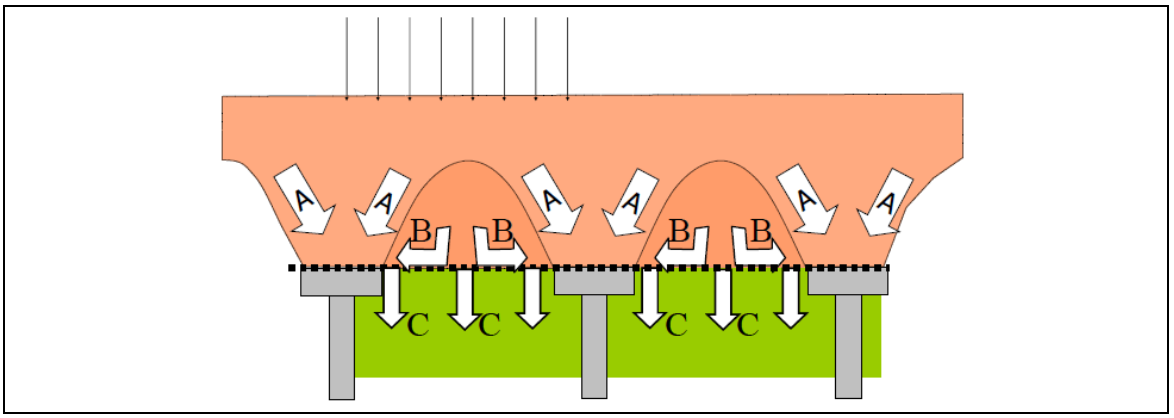

Figure 24: Load distribution in a piled embankment (Van Eekelen and Bezuijen, 2012)

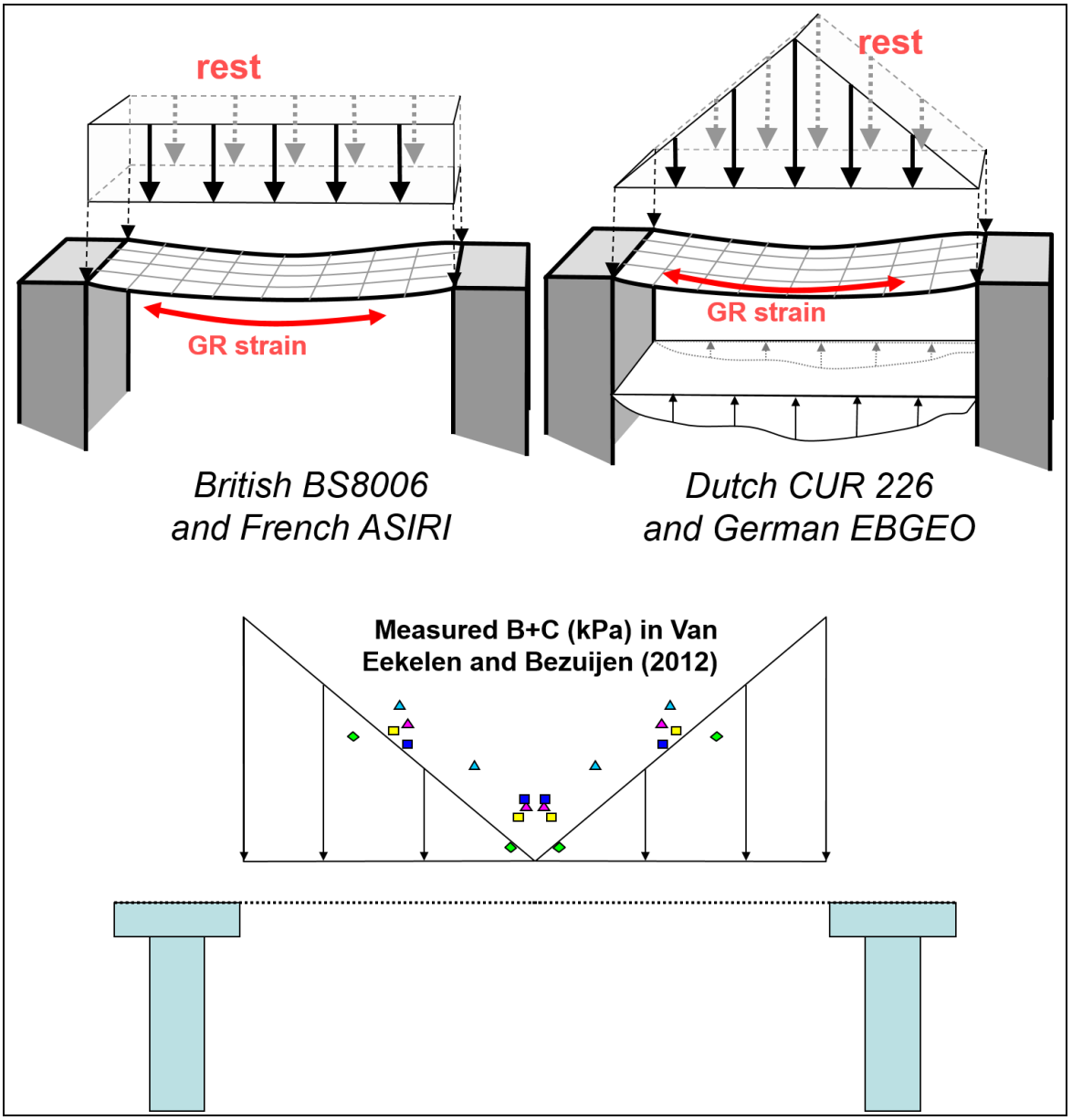

Figure 25: Measured load distribution on a geosynthetic reinforcement strip in a piled embankment, from Van Eekelen and Bezuijen (2012) and comparison with the theoretical load transfer distributions proposed in the different design approaches: British standard BS 8006, ASIRI project (IREX, 2012), CUR-rapport 226 and German standard EBGEO

3. NUMERICAL MODELING OF RIGID INCLUSIONS

Whilst numerical methods have progressively become the most popular analysis technique, their results are only as good as the model and the input parameters used for the computation. Moreover blind implementation of such tools without a deep understanding of the modeling process and suitability of the characteristic parameters may lead to unforeseen disastrous consequences.

Currently, finite element modeling (FEM) and the finite difference methods (FDM) are globally the most used numerical methods. Both methods are implemented to solve the hydro-mechanical equations governing engineering problems (in this case the foundation solution involving a load transfer platform and rigid inclusions) considered as a continuous medium. The FEM and FDM methods allow the verification of the bearing capacity and the stability for the modelled geotechnical application. Nevertheless, the relevance and the accuracy of the numerical results will depend on the relevance of the constitutive models, on the representativity of the input values adopted for the various material properties and on the selection of well-suited mesh generation procedures. As underlined in IREX (2012), the numerical results obtained through these methods yields an approximated solution whose relevance and accuracy depend on:

- the model constitutive laws of materials and interfaces,
- the mesh generation strategy (discretization of the medium) with the use of finer meshing pattern at the locations where larger strain field variations are expected,
- the type of elements adopted (number of nodes) and the interpolation laws for each element (e.g. linear vs. quadratic),
- the use of interfaces between the structural elements and the soil in order to allow the integration of soil/structure interaction phenomena;
- and the boundary conditions.

It is the authors' experience that the use of FEM is well-suited for studying the problem when displacements are small. For large displacements (close to failure or instability), the use of simulations, including strong "large displacement" assumptions and procedures, becomes necessary (e.g. FDM or the most-recent developed Material Point Method, called MPM, which is to become soon available in the commercial software Plaxis 3D).

A great advantage of the numerical methods in ground improvement solutions with rigid inclusions is the ability to perform parametric studies to optimize the design pattern, especially the height and properties of the load transfer platform and the quantity and geometrical pattern of the rigid inclusions.

Considering the Dutch and French guidelines (respectively the CUR-rapport 226 and the ASIRI project report of IREX), the numerical simulations can be conducted with 2D or 3D modeling. According to IREX (2012), implementation of 2D simulations can be performed with axisymmetric or plane strain models; both of which have drawbacks. With the axisymmetric configuration, it is only possible to model a single unit cell (the influence area of an inclusion is considered as a circle) that is located near the embankment axis. However, the three dimensional inclusion must be transformed into an equivalent 2D plate in plain strain modeling. In this type of configuration, the rows of inclusion are transformed into "walls" perpendicular to the sectional plane of the model. Moreover, in 2D models, rigid inclusions may be represented by either volumetric or beam elements. According to the guidelines of IREX (2012), it is preferable to model the rigid inclusions using volumetric elements.

Nevertheless, even if 3D models have the advantage of providing a global view of the problem's geometry, the high computational time necessary to obtain results for each phase of the project leads the designers to parsimonious use of 3D simulations in the case of a particular asymmetric geometry, a reinforced slope, a footing subjected to complex (dynamical) loading or non-uniform loads applied to slabs on grade. The use of 2D and 3D models is discussed in CUR-rapport 226. Interested readers can additionally refer to Slaats and van der Stoel (2009) who have conducted a comparative study using Plaxis 2D and 3D to model a piled embankment with rigid inclusions submitted to lateral forces.

IREX (2012) provides practical guidelines for numerical modeling with consideration of the following points:

- the definition of the geometric boundaries of the studied domain and the boundary conditions,
- the definition of the constitutive models regarding:
    - the identification of the parameters of the problem,
    - the hydro-mechanical characteristics of the soils, the load transfer platform, the rigid inclusions and the potential geosynthetic reinforcements,
    - the characteristics of the inclusion/soil interfaces,
    - and the characteristics of the slab on grade or raft,
- and consideration of the construction phases.

Ideally, the numerical model has to be calibrated on the basis of *in-situ* testing (with soil characterization results and if possible, the results of a static load test performed on a rigid inclusion).

As underlined in IREX (2012), the realization of numerical calculations has to be performed in large deformations if geosynthetic reinforcement elements are considered in the problem (second-order effect).

For the purpose of obtaining relevant numerical results, the results must always be considered with consideration of:

- the basic geotechnical assumptions of the computation model,
- the constitutive models and parameter values used for the different materials (including their drained or undrained behavior),
- the incertitude related to the execution mode (probably the most difficult aspect to be assessed in that kind of problem),
- the different construction phases,
- the long-term behavior of the construction with
    - the use of long-term parameters for the various materials (e.g. the product isochrones curves of the geosynthetics taking into account the duration of the loading and the lifetime of the structure to be supported),
    - the consideration of the consolidation effects.

A particularity of the numerical methods for the rigid inclusion solutions is the modeling of the inclusion/soil interface. First, the mesh has to be refined along the inclusion/soil interface. Second, the constitutive model of the interface has to be considered in detail. As reported in IREX (2012), the constitutive models typically used for interfaces are of the elastoplastic type. The elastic part allows the modeling of a gradual mobilization of shear with strain. Two techniques are used for the plastic part:

- either a reduction of ϕ' and c' is applied,
- or a fictitious soil with $\phi' = 0$ and with a nonzero cohesion for simulating constant friction $c'=q_s$, in compliance with the limiting values of shaft friction, e.g. as set forth by the French standard for deep foundations NF P 94-262.

It is to note that this kind of approach should only be conducted by a very experienced geotechnical engineer, as the use of soil parameters, which do not have a physical specific and special interpretation can be a very dangerous practice. This particular approach was recently followed by Racinais (2015) who calibrated soil parameters of a rigid inclusion problem on the Frank and Zhao friction curves (1982) to obtain better simulations of the rigid inclusion behavior using Plaxis software. Racinais (2015) presented his numerical model using a case history (plate load test performed on a rigid inclusion in Venette, France).

Another possibility to design rigid inclusion concepts is the use of homogeneization methods that are only applicable to vertical loadings. In this method a typical representative unit cell that includes a typical inclusion, its peripheral soil and load transfer platform volumes is modeled. This unit cell is generally modeled using an axisymmetric model, and is then compared with a second model that has similar dimensions but in which the soil and inclusion are replaced with a single homogeneous material. The characteristics of this material are chosen in such a way to obtain similar results than with the first model. As highlighted in IREX (2012), this equivalence is typically verified by matching the settlements and defining an apparent modulus E^* for the homogeneous material. The use of this apparent modulus E^* is then extended to model the entire geometry of the problem.

One of the drawbacks of this approach is that it does not consider inclusion/soil interface behavior. The introduction of a correction coefficient, denoted by β, in the definition of E^* can be used in a first approximation to integrate the interaction at the interface:

$$E^* = \frac{\left(\frac{E_p A_p}{\beta} + E_s A_s\right)}{A} \tag{32}$$

where E_p is the deformation modulus of the rigid inclusion, A_p is the rigid inclusion area, E_s is the deformation modulus of the soil, A_s is the soil area and A is the total considered area. β is thus a correction coefficient modelling the effect of the inclusion/soil interaction (the sliding behavior between both materials at the interface) on the apparent modulus.

A more complex homogeneization method, called the extended biphasic modeling, has been developed to model the inclusion/soil interface with more accuracy. This method considers the inclusion/soil interaction and the modeling of shear and bending forces in the rigid inclusions (Sudret and de Buhan, 2001; Cartiaux *et al.,* 2007; Hassen *et al.,* 2009; Cuira and Simon, 2009; Thaï Son et al., 2009 and 2010).

Regarding the numerical modeling of the load distribution in the load transfer platforms, Van Eekelen et al. (2013) cite the works of Le Hello and Villard (2009). Le Hello and Villard (2009) focused on load

transfer mechanisms of piled embankments and presented the results of numerical and experimental studies focusing on the topic of the load distribution. Within this framework, they developed an advanced numerical model combining 3D Discrete Element Method (DEM) and the Finite Element Method (FEM), and obtained numerical results for the load distribution in line with the concentric arches model of Van Eekelen et al. (2013).

4. EXECUTION PROCESSES FOR THE REALIZATION OF RIGID INCLUSIONS

4.1. Execution methods for the installation of rigid inclusions

As previously mentioned, typical rigid inclusions are concrete columns (possibly installed in the ground using classical or adapted piling techniques), grout and jet grout columns, soil mix elements (columns, panels, trenches, blocks…), Controlled Modulus Columns (CMC), grouted stone columns, etc. A list of rigid inclusions is given in the Table 5 and illustrated in Fig. 26.

Providing a large description of construction processes, the State of the Art Report of Chu et al. (2009) can be consulted to obtain general information and references concerning all these techniques.

Table 5 does not include typical piling methods – as they are not directly considered as ground improvement methods – and does not cover deep mixing and jet grouting inclusions – as they are part of the category D of ground improvement methods dedicated to grouting type admixture techniques. Nevertheless the realization of rigid inclusions with classical (or adapted) piling methods and with deep soil mix or jet grout elements certainly represents a growing market in the field of the foundation engineering.

Table 5. Types of rigid inclusions according to Chu et al. (2009)

Method	Description/Mechanisms	Advantages	Limitations
Controlled modulus columns (CMC)	A borehole is formed by pressing and a column of 250 to 450 mm in diameter is formed by pressure-grouting.	The strength and stiffness of the columns can be controlled. The method produces nearly no spoil or vibration.	Need special installation machine
Multiple stepped pile	A borehole is locally enlarged by an opening tool so a column formed by grout or concrete will have enlarged steps at a given interval.	Increase the capacity of grout or cast *in-situ* concrete column without incurring much higher cost.	Used only for soil where an unsupported borehole can be formed.
Grouted gravel or stone column	A column is formed by forming a gravel or stone column and then grouting it from the bottom upward using a preinstalled grouting tube.	Increase the strength of gravel or stone columns considerably by increasing the stiffness of the columns and the interface friction	Expensive. Quality control may be difficult
Vibro-concrete column	Concrete is used to form a column using a method similar to that for bottom-feed dry stone columns.	Can be used where stone columns are not suitable. An enlarged bottom can be made.	Difficult to control the uniformity of the column
Cast-*in-situ*, large diameter hollow concrete (PCC) pile	A large diameter (1 to 1.2 m), hollow concrete pile is cast *in-situ* using a form of two cylindrical casings inserted into ground.	More economical and better quality control than stone columns, cement mixing piles or concrete piles	Need special installation machine
Y or X shaped pile	A grout or concrete pile is formed by inserting a Y or X shaped casing as a form into ground.	Saving cost without compromising bearing capacity compared with the circular pile of the same diameter	Need special installation machine

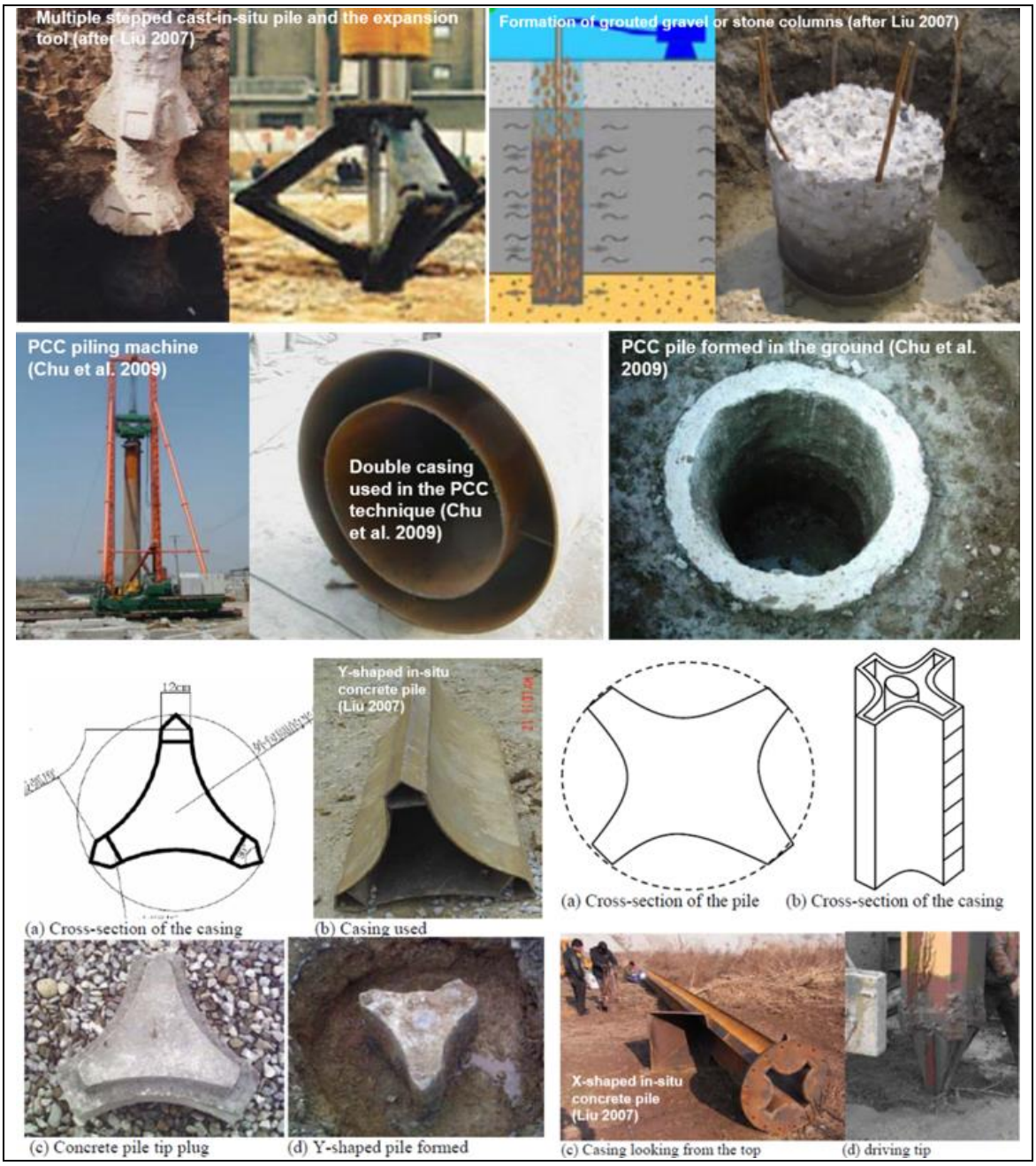

Figure 26: Different types of rigid inclusions, from Chu et al. (2009) and Liu (2007)

For the deep mixing method, the interested reader can refer to the following State of the Art references: Bruce et al. (1998), Porbaha (1998), Holm (2000), FHWA-RD-99-167 (2001), CDIT (2002), Eurosoilstab (2002), Terashi (2003), Topolnicki (2004), Larsson (2005), Rutherford et al. (2005), Essler and Kitazume (2008), ALLU (2010), Denies and Van Lysebetten (2012), Kitazume and Terashi (2013), FHWA-HRT-13-046 (2013) and GeotechTools (2013), Denies and Huybrechts (2015). For the design of soil mix elements with a bearing function, the designers can refer to the SBRCURnet/BBRI soil mix handbook (2016).

For jet grouting columns, the reader can refer to Shibazaki (2003), Essler and Shibazaki (2004), Croce et al. (2014), Burke (2012) and to the practical guidelines of Maertens et al. (2016).

Within the framework of the present keynote, the authors have still chosen to illustrate the execution of rigid inclusions within the framework of practical projects involving the CMC and the deep mixing techniques.

4.2. Controlled Modulus Columns (CMC) used as rigid inclusions

4.2.1. Execution of Controlled Modulus Columns (CMC)

As shown in Fig. 27 and 28, a Controlled Modulus Column (generally called CMC) is installed in soft ground using a specially designed auger that is composed of a penetrating helical tip and a cylindrical-like hollow stem follow-up section. As the auger is thrust and screwed into the soil, the cylindrical extension displaces the soil laterally, and reduces the amount of spoil that is generated to negligible amounts compared to cast *in-situ* piling solutions such as continuous flight auger (CFA) or bored piles. During the auger extraction, grout is pumped through the hollow stem and auger to form a columnar inclusion with a diameter that is usually 250 to 450 mm. The strength of the columns can be controlled by varying the strength of the grout.

The CMC rig should be able to provide a continuous down pull with a high torque in rotation. The torque is typically in the range of 20 tm, continuous pull down is in the range of 20 t, and rotation speed is in the order of 15 rpm. Further enhancements to the equipment can include a radio control unit to allow the rig operator to directly command the concrete pump from his control panel. The control panel displays torque, speed, depth, down pull force, grout pressure and volume of pumped grout.

4.2.2. Advantages of Controlled Modulus Columns (CMC)

Unlike stone columns whose stability relies on the horizontal containment of the soil (Barksdale and Bachus, 1983) or deep soil mixing where column strength is dependent on the *in-situ* soil properties, CMCs do not rely on external parameters for lateral stability nor are their strengths affected by the surrounding soil. In fact, column strength can be controlled simply by varying the strength of the grout. Thus, this method can reduce settlements more efficiently compared to other techniques in which inclusions are installed in the soil.

As the deformation moduli of CMCs are typically 50 to 3000 times that of the weakest soil stratum (Masse et al., 2009), it is possible to reduce ground settlements using a lower replacement ratio in comparison with inclusions that are composed of granular materials (Murayama, 1962 and Aboshi et al., 1979).

An advantage of the CMC technique, in comparison with stone column type or grouting type techniques, is its production rate. In order to reach the required size, mixing degree or strength, the ground improvement techniques involving discontinuous additives (e.g. stone columns) or grouting type admixtures (e.g. jet grouting or deep mixing) will be time-consuming in comparison with the CMC technique. For example, introducing and compacting stones for the construction of stone columns must be carried out in numerous lifts, and time must be allocated to sufficiently enlarge the column and compact the stones in each lift. Similarly, grout that is produced for jet grouting or deep soil mixing be must progressively mixed with the soil in place (sometimes with considerable amounts of penetration and withdrawal phases in the case of the soil mix technique e.g.), which will result in a lower production rate.

CMC grout or concrete is produced in a concrete batching plant, and placement of the material is performed with the same production rate as obtained for the CFA piling technique.

The amount of vibration that is generated by CMC installation is comparable with CFA piling as the installation process itself is vibration free. This characteristic can make CMC the preferred choice over vibratory ground improvement techniques.

The main advantages of CMCs can thus be summarized as:

- strength independency from *in-situ* soil,
- generally high settlement reduction with lower replacement ratios in comparison to other ground improvement techniques with additives or inclusions,
- independent from external parameters for lateral stability,
- vibration free installation process,
- installation with lateral displacement of the soil involving negligible volumes of spoil in comparison with *in-situ* cast piling systems,
- and high installation rates.

Figure 27: Photography of a CMC auger

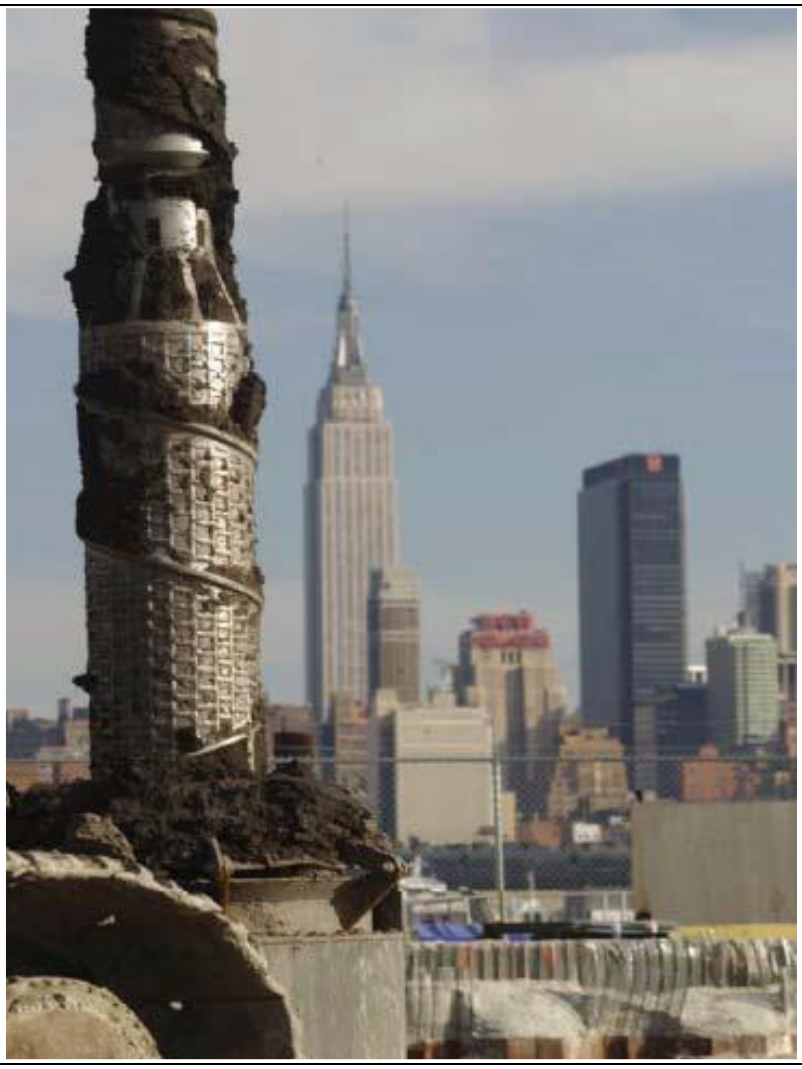

Figure 28: CMC auger used for CMC installation, from Chu et al. (2009)

4.2.3. Case histories relating to the use of Controlled Modulus Columns (CMC)

4.2.3.1. Previous world records for the installation depth of CMCs

In 2006, the CMC method was used for the foundation system of WeeHawken residential resort opposite Manhattan along the Hudson River in New Jersey, USA. This site had very poor soil conditions with miscellaneous heterogeneous fills over a thick layer of soft, highly compressible organic clay. The displacement auger that was used in this project is shown in Fig. 28 and 29. A very large piling rig was used to install 2100 CMCs with depths varying from 21 m to 30 m, which was the deepest installation depth for CMC in the world at that time.

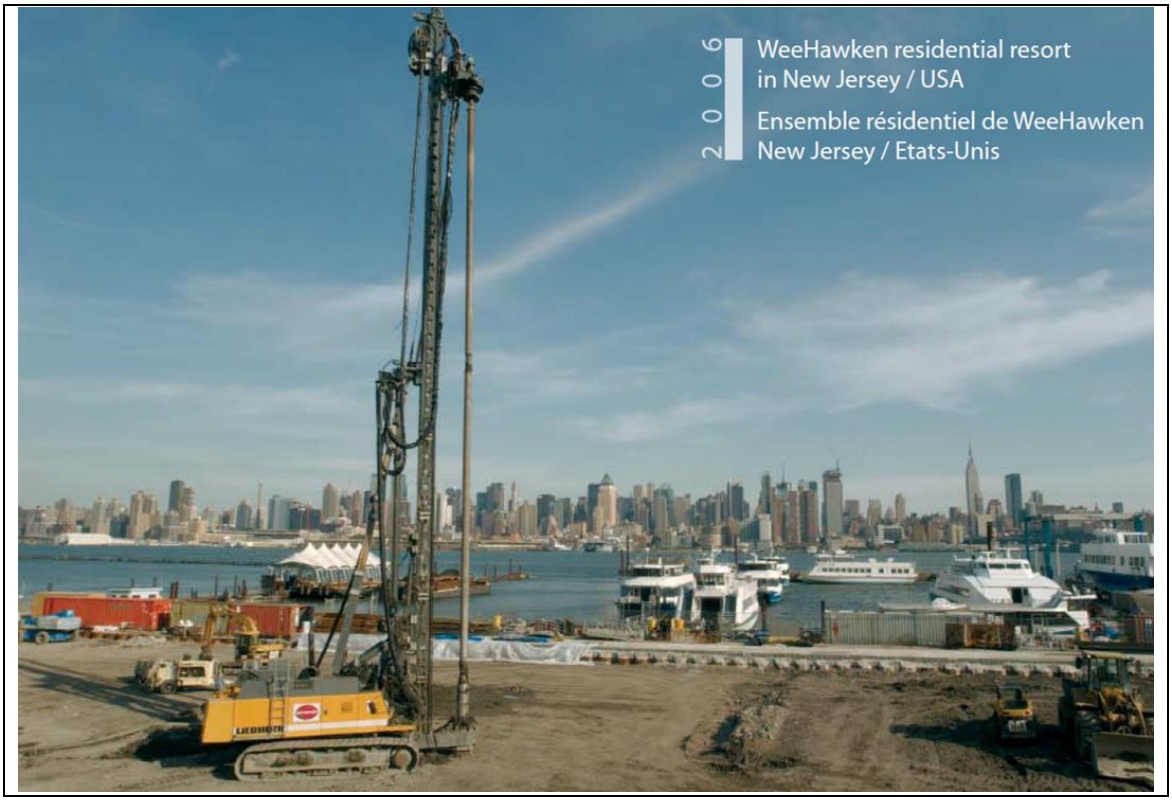

Figure 29: CMC installation on the construction site of the WeeHawken project in New Jersey, with the courtesy of Menard Company

This world record was broken a few years later with the installation of CMCs in Louisiana, USA. Buschmeier et al. (2012) have reported the installation of 34 m long CMCs to support oil tanks. As part of the development of an oil terminal located on the banks of the Mississippi River in New Orleans, five steel tanks, each 12.8 m high have been constructed. Three tanks had diameters of 39.6 m and the two other tanks' diameters were of 45.7 m. The maximum pressure that the tanks exert to the ground is 130 kPa, and an additional pressure of 16 kPa can be added due to the installation of the load transfer platform.

The superficial fill layer of the load transfer platform that is approximately 0.15 to 1.2 m thick is underlain by soft to medium stiff silty clay (presenting some traces of organic matter and localised sand pockets), which extends to depths varying between 4 and 6 m. This layer is followed by very soft clay (with a silt and sand content) reaching depths ranging between 20 and 24 m. A thin sand layer was also identified at approximately 21 m depth. Medium stiff to stiff clay (with fine sand pockets and shell fragments) was observed up to 32 m depth followed by stiff to very stiff silty to sandy clays over a very dense layer of silty sands at a depth of about 34 m. The groundwater level was located at less than 1 m below the ground level.

Project specification stipulated tanks' maximum and central settlements as given in Table 6.

Table 6: Tank Performance Criteria (Monitoring Period = 3 years after hydrotest)

Tank	**Center Deflection**	**Tank bottom settlement**	**Uniform Settlement**
Steel bottom	100 mm	50% of API 653 Standard	200 mm

CMCs were installed with a higher replacement ratio down to the depth of about 21 m where a sand layer with reduced compressibility was identified, and with a lower displacement ratio down to the maximum treatment depth at about 34 m. Figure 30 illustrates the installation of the CMCs on the construction site.

Due to the variations of the soil profile, it was necessary to design each tank individually. As shown in Fig. 31, analyses included three dimensional digital modeling of a quarter of a tank, three dimensional modeling of a thin slice of the tank and analytical calculations of rafts on floating piles. Details and results of the numerical simulations are given in Bushmeier et al. (2012).

Figure 32 presents a schematic view of the 3D slice model concept finally used for the design of all the tanks. As a result of these numerical analyses, CMCs were installed to depths of 21 and 34 m with diameters that were respectively 318 and 470 mm. Installation depth was variable for each tank.

Figure 30: Installation of the CMCs on a construction site (oil terminal) located on the banks of the Mississippi River in New Orleans, USA

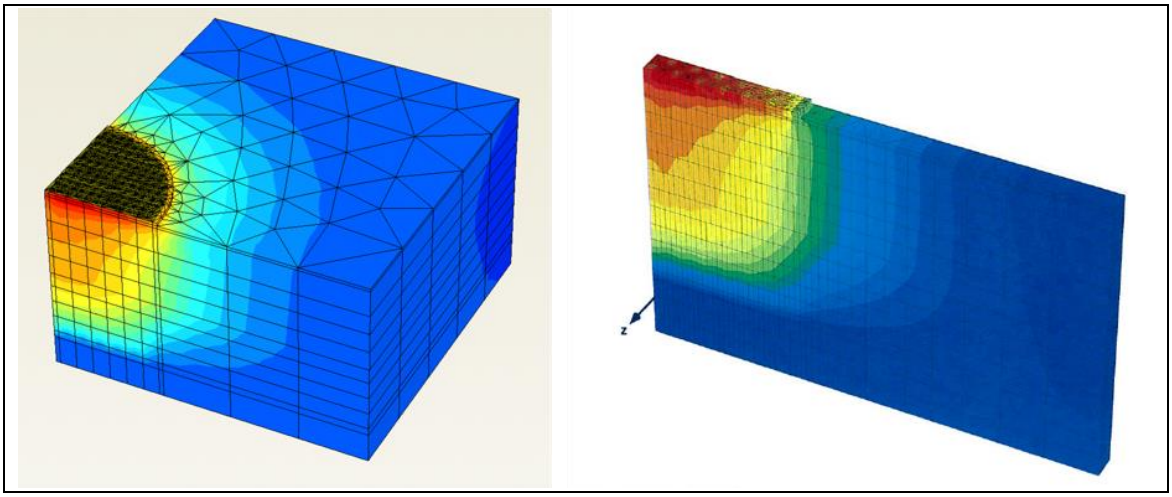

Figure 31: Results of 3D FEM analysis for quarter of tank model (left) and thin slice model (right), from Buschmeier et al. (2012)

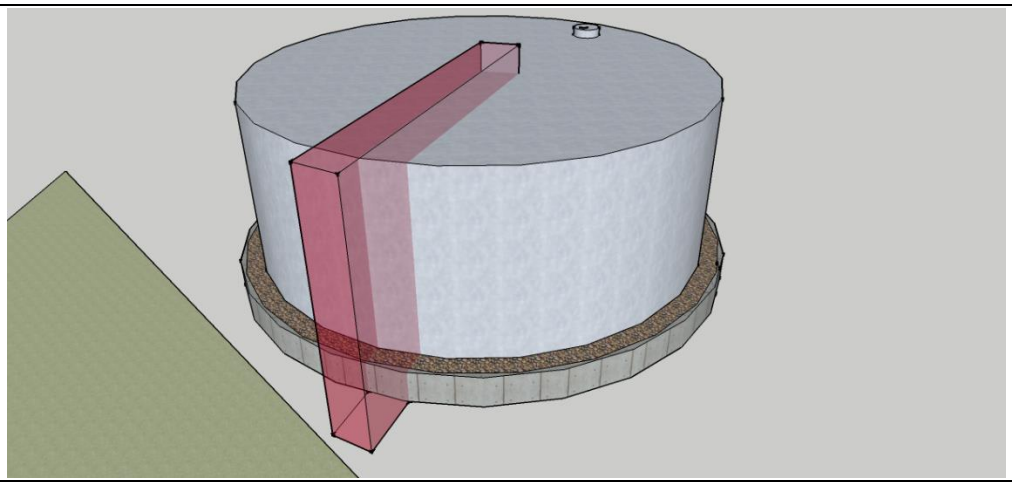

Figure 32: 3D thin slice model concept used for the design of all the tanks, from Bushmeier et al. (2012)

4.2.3.2. Current world record for the installation depth of CMCs

Hamidi et al. (2016) have recently reported the installation of 42 m long CMCs that, to the knowledge of the authors, are the world's deepest CMCs ever executed. This project is also located near New Orleans, and includes four oil tanks, a water tank, two shop and maintenance buildings and ancillary structures. The diameter and height of the oil tanks are respectively 43.3 m and 11 m, and each tank will be filled with a product that will apply a design pressure of 120 kPa to the bottom of the tank.

Prior to construction, the site was relatively level and approximately at elevation ±0 m RL (reduced level). Initially, the uppermost 0.3 m of the ground was treated and modified to cement-stabilised clay. The site was then elevated with sand to +1.2 m RL. The tanks will be built on a pad that has been further raised by 0.3 m.

The upper 1.5 to 3 m thick layer of ground consisted of a crust of desiccated over consolidated clay with an over consolidation ratio (*OCR*) of 4. Below this layer was a very soft clay layer that extended to depths of approximately 33.5 m. The *OCR* for this layer was assumed to decrease with depth from 3 in the upper part to 1.2 in the lower layers. A sand layer was present at depths of approximately 33 m to 36 m in some areas, but in other areas this layer was replaced by a stiff to medium stiff layer of clay roughly up to depths of 51 to 57 m. This lower clay was understood to have an OCR of 1.1. Cone penetration test (CPT) profiles at the location of the four tanks showed that the cone resistance was almost consistently very low and negligible in the soft clay. The CPT and soil profile of one of the tanks in shown in Fig. 33.

Initial calculations indicated that the tanks were susceptible of undergoing settlements in the magnitude of 1.5 m to 1.8 m without implementation of an improved foundation system.

Since expected settlements exceeded the tank's design criteria, limiting long term settlements under the tanks to 300 mm and differential settlements to the values specified in API 653 (2001), specific geotechnical measures had to be implemented. The specialist contractor who was awarded the project proposed that three oil tanks be supported at the edge by a concrete slab and a geotextile-reinforced gravel ring wall while the fourth tank was designed to be supported by a load transfer platform and a geotextile-reinforced gravel ring wall. All structures were to be supported by square grids of CMCs with typical centre to centre spacing of 1.7 to 2.5 m and diameters of 396 mm.

The design included an iterative approach and finite element analyses using a combination of three different modeling techniques; i.e. axi-symmetrical modeling, three dimensional strip modeling, three dimensional global modeling. The calculation process was iterative as parameters needed to be adjusted in such a way that the various types of models yielded similar results. The purposes of these various computational models are described in Hamidi et al. (2016). This approach led to approximately 280 mm of long term settlement under the centre of the tank, of which, 75% occurred below the toes of the CMCs rather uniformly.

As a result of the numerical analyses, more than 2600 CMCs were installed under the structures to an average depth of 36.5 m during a period of approximately 4 months.

Installing CMCs, with a specially adapted equipment presenting a drilling capacity up to 45m depth, down to the depth of approximately 42 m in this project has increased the world record described in Bushmeier et al. (2012) by 8 m.

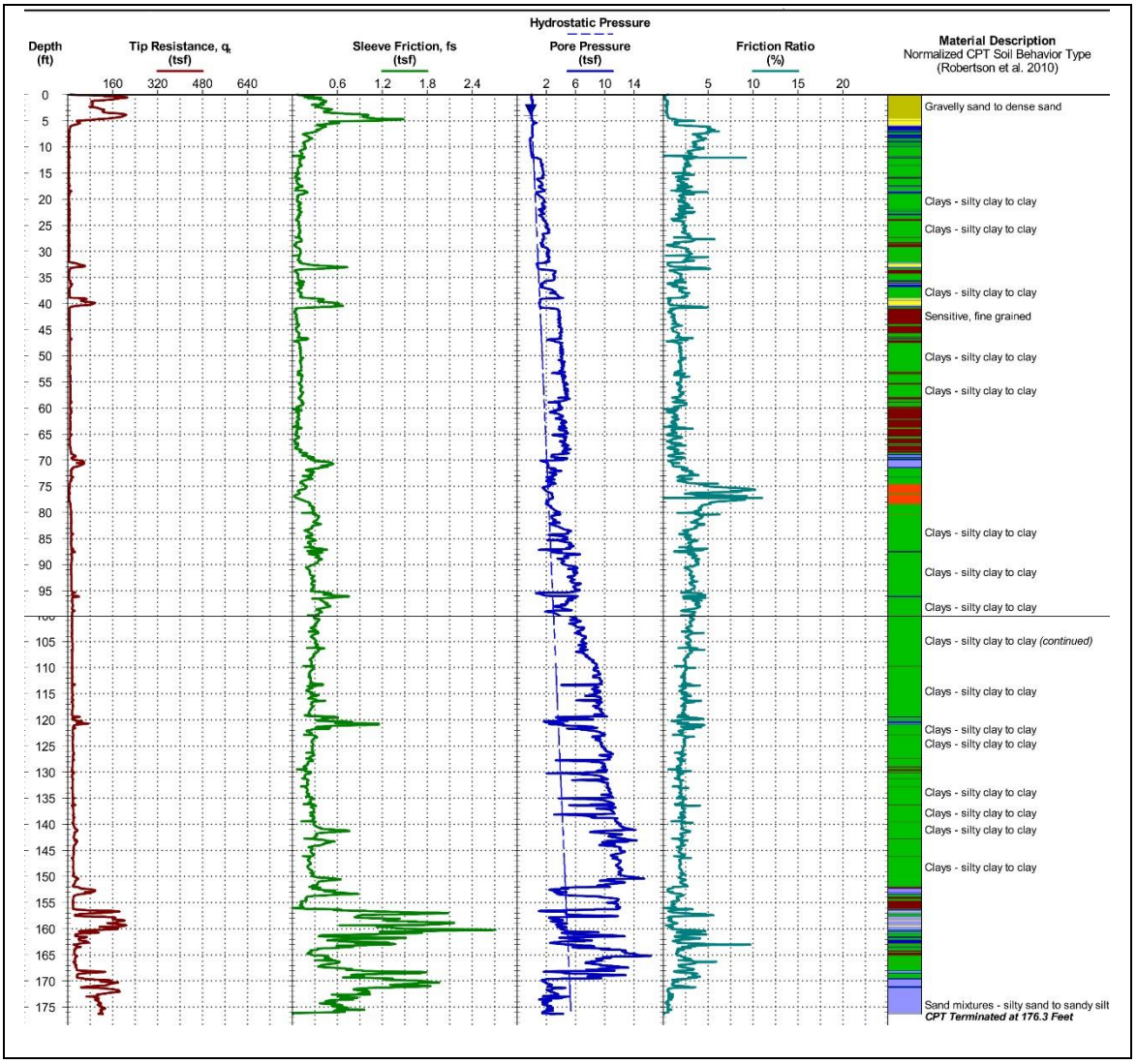

Figure 33: CPT and soil profile of one of the tanks (note: units in empirical system)

5. HYBRID CONCEPT OF FOUNDATIONS WITH RIGID INCLUSIONS INSTALLED WITHOUT LOAD TRANSFER PLATFORM

5.1. Case history – construction of an eleven-story building in Leuven (Belgium)

5.1.1. Introduction to the project: the REGA-Instituut (KU Leuven)

The present case history illustrates the use of soil mix panels as an alternative to pile groups for the foundation of an eleven-story building in Leuven (Belgium).

This building is the REGA-Instituut of KU Leuven. A few years ago, the university has actually decided on the construction of a new laboratory for microbiology and medicinal chemistry. The project consisted of a L-shaped building, such as illustrated in Fig. 34. The project includes a lot of laboratory facilities, an animal house, several offices, an underground parking, a lunch room, meeting rooms and a 180-person amphitheater. The construction of this L-shaped building is complicated by the realization of an underground tunnel (for the supply of the laboratories) connecting the REGA-Instituut to an adjacent research building of KU Leuven.

Figure 34: Project presentation for the REGA-Instituut of KU Leuven - with the courtesy of SVR-Architects

5.1.2. CSM-panels used as bearing elements as alternative to pile groups

Originally, the foundation of the building consisted of a number of pile groups supporting the columns or pillars of the building frame. Figure 35 presents a schematic view of a part of the initial foundation plan. The pile groups supporting the pillars of the building frame are represented on the foundation plan as well as the "supply" tunnel. At the beginning of the project, this concept was discussed and an alternative was proposed with the installation of soil mix panels (realized with the CSM technique) as a replacement for the pile groups. Indeed, this solution was cost-effective and presented the advantage to decrease the constraints related to the consideration of the (potential seismic) lateral loads imposed in the design requirements and job specifications for the building.

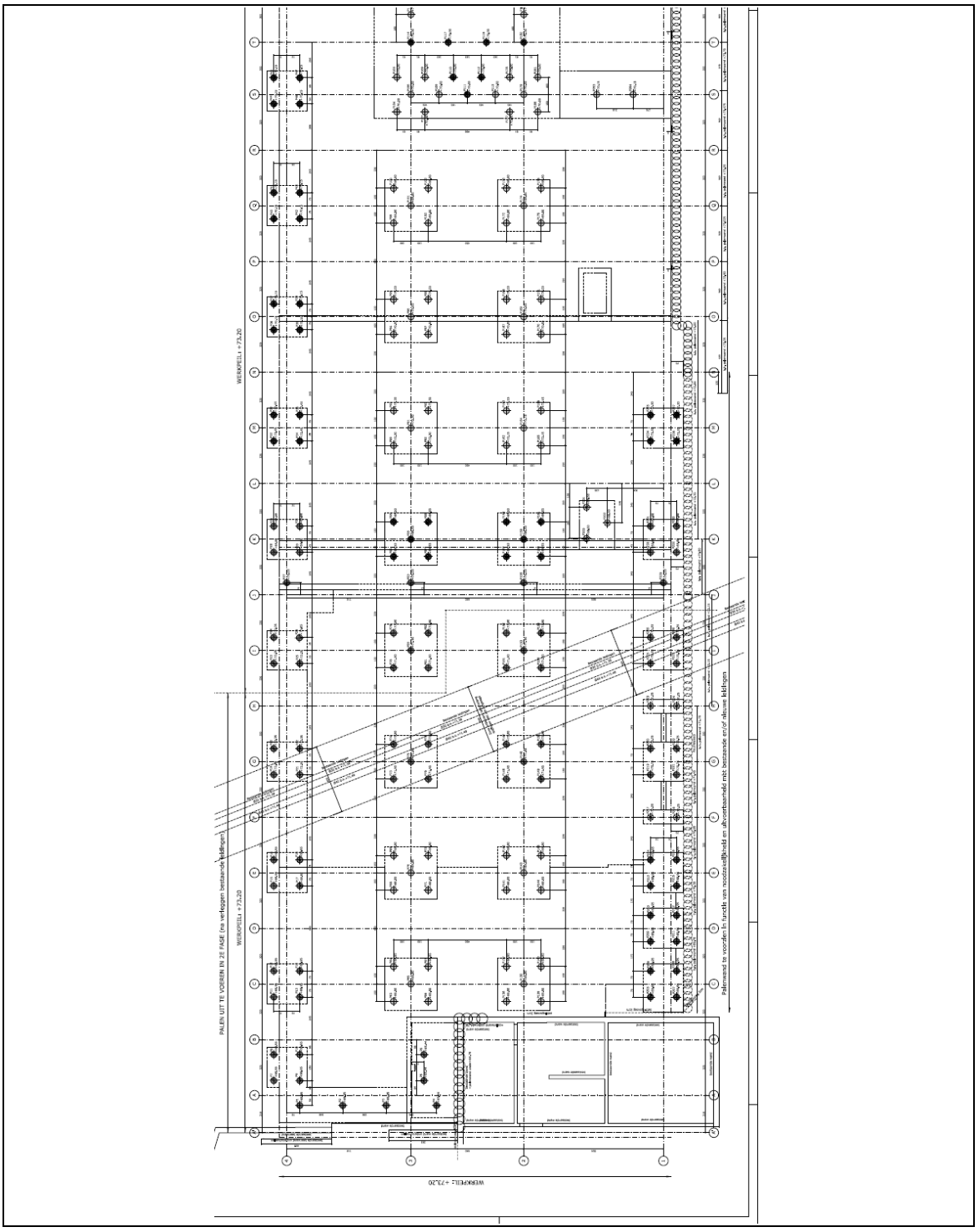

Figure 35: Schematic view of a part of the original foundation plan of the REGA-Instituut with the different pile groups supporting the pillars of the building frame and the connection tunnel

Figure 36 presents the new concept of foundations made of CSM-panels. As illustrated in Fig. 36, unique, double and triple adjacent CSM-panels were executed in place of the pile groups. In the following paragraphs, the terminology "CSM-bearing elements" is used to describe the three foundation patterns (unique, double and triple CSM-panels). Figure 37 presents an aerial view of the construction site during the foundation works. Figure 38 presents two views of the CSM-panel caps after execution during summer 2013 by the Belgian company Soetaert nv.

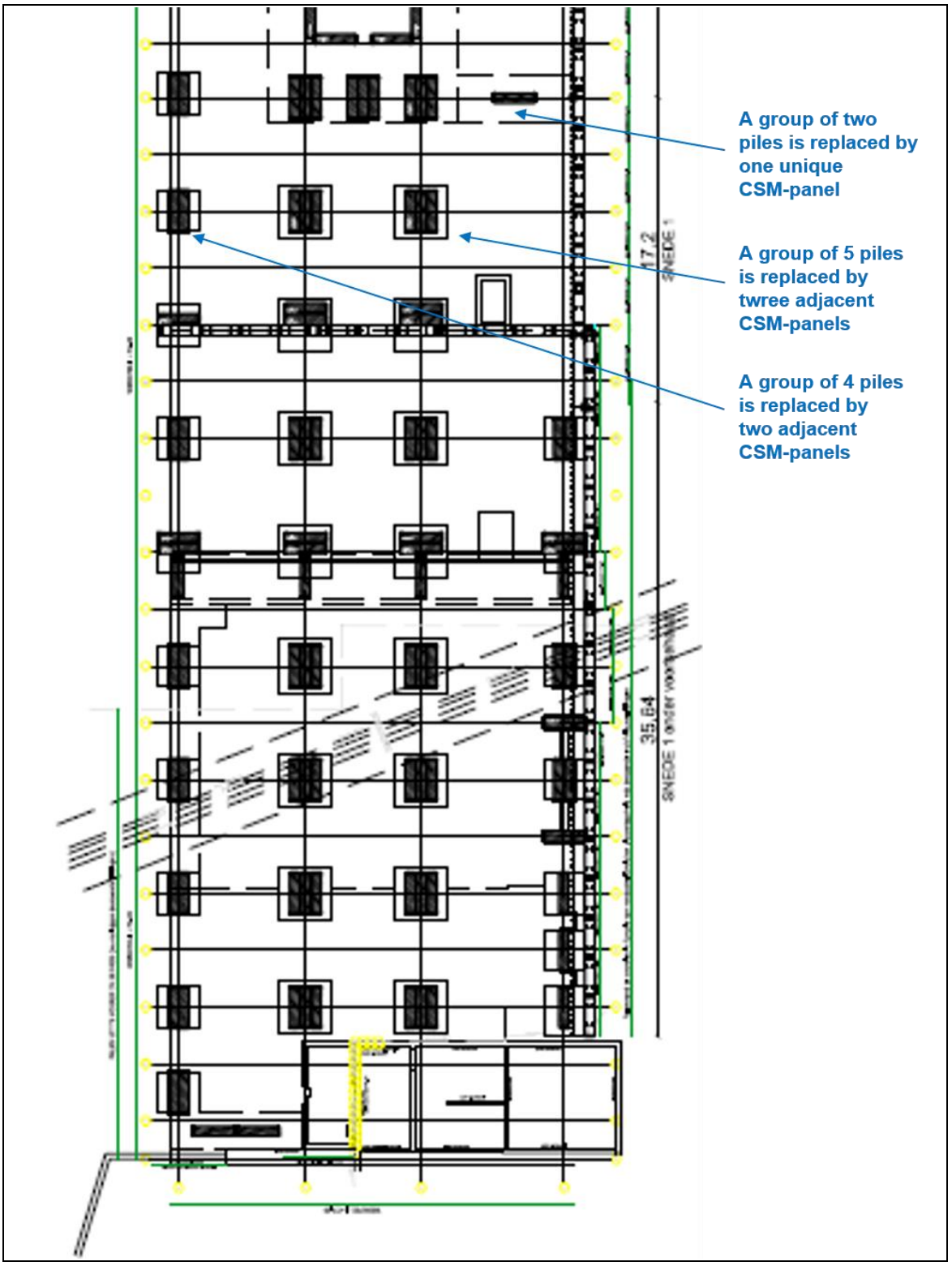

Figure 36: Schematic view of a part of the new foundation plan of the REGA-Instituut with the different soil mix panels (CSM-panels) supporting the pillars of the building frame and the connection tunnel

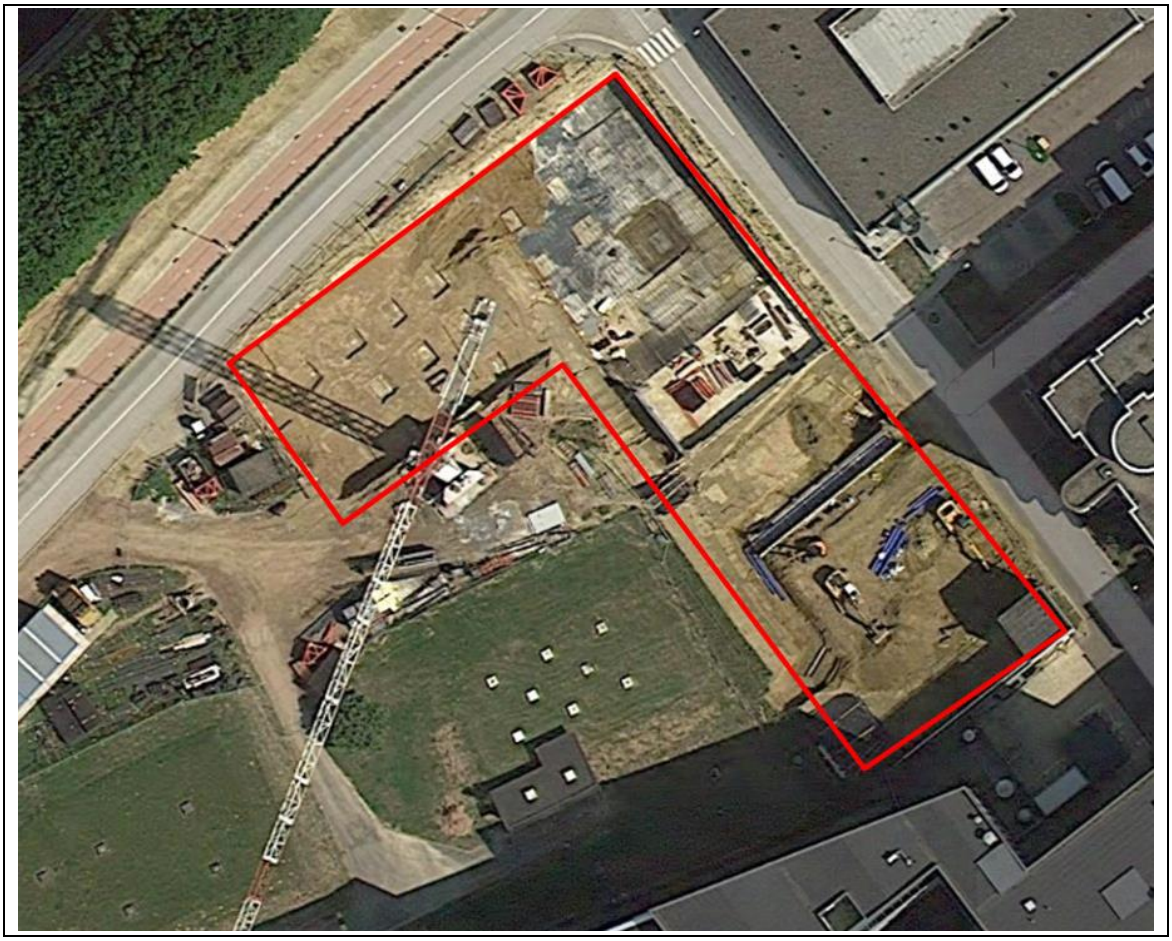

Figure 37: Aerial view of the construction site during the execution of the foundation works (Google view in July 2013)

Figure 38: Different views of the CSM-panel caps after execution during summer 2013

5.1.3. Design of the CSM-panels as bearing elements

The design of the CSM-bearing elements will be performed as follows. First, the CSM-bearing elements were not directly connected to the slabs of the building pillars allowing lateral movements on the top of the soil mix panels in case of seismic lateral loading. No rigid connections with steel reinforcement is thus foreseen between the tops of the CSM-bearing elements and the slabs supporting the building pillars. The CSM-panels were therefore mainly designed to support vertical compressive loads. For that reasons, no steel reinforcement was placed in the different CSM-bearing elements during execution.

Considering the structural design of the CSM-bearing elements, it was imposed that the UCS design value of the soil mix material was always larger than the structural vertical stress (mainly due to the weight of the building): $f_{c,d} > q$. The design value of the UCS of the soil mix material was verified with the help of lab tests performed on cored samples (the boreholes are visible in Fig. 38 at the top of several CSM-bearing elements). A vertical coring on the full depth of, at least, one CSM-bearing element was required in order to control the UCS of the soil mix material until the base of the bearing element. The design methodology of BBRI, presented in Section 2.2.4.3 of the present keynote, was followed for the computation of $f_{c,d}$.

The geotechnical design of the CSM-bearing elements was verified only considering the base resistance of the element. This base resistance (= toe resistance) was computed on the basis of CPT results according to the De Beer procedure, as required in the Belgian National Annex of Eurocode 7 for piles (see Rapport 12 of BBRI). No shaft resistance was considered in the calculation of the bearing capacity of the different CSM-bearing elements. According to this design approach, the different CSM-bearing elements were considered as a pile foundation with only the base resistance acting in the computation of the bearing capacity. That assumption will be later discussed considering the dimensions of the different CSM-bearing elements.
Figure 39 presents the different design configurations for the installation of the unique, double and triple CSM-panels. The three diagrams present the variation of the cone resistance, q_c (MPa), and the base resistance, q_b (MPa), computed according to the De Beer approach, as a function of the depth respectively for the three patterns (unique, double and triple). The q_c-curve is therefore the same on the three diagrams; only the q_b-curve varies as a result of the different dimensions of the CSM-bearing elements.

According to the rapport 12 of the BBRI (2009), the base resistance (R_b) was computed for each CSM-bearing element as follows:

$$R_b = \epsilon_b q_b A_b \alpha_b \beta \tag{33}$$

where ε_b (-) is different from 1 in tertiary clay (in the present case, the CSM-panels are installed in tertiary sand: $\varepsilon_b = 1$), A_b (m²) is the pile base, q_b (MPa) is the base resistance according to the De Beer approach, α_b (-) is an empirical factor depending on the execution process (in this case $\alpha_b = 0.5$ as for the bored piles) and β is a shape-factor taking into account the shape of a non-circular pile base:

$$\beta = \frac{1+0.3\frac{B_2}{B_1}}{1.3} \tag{34}$$

where B_1 and B_2 are respectively the longer and the shorter side of the pile base.

A design value for the bearing capacity, $R_{c,d}$, (only based on the base resistance) was then computed according to the principle of Eurocode 7 (with the application of the different partial factors) and this value was compared, for each CSM-bearing element, with the vertical compressive stress due to the structural loads:

$$R_{c,d} = \frac{R_b}{\gamma_b \gamma_{rb} \zeta} < q \tag{35}$$

where γ_b is the partial factor on base resistance (in this case: $\gamma_b = 1.35$), γ_{rb} is the model factor (in this case: $\gamma_{rb} = 1.15$) and ζ is the correlation factors taking into account the density of the soil tests on the construction site (in this case: $\zeta = 1.2$).

For example, considering a triple CSM-bearing element (as represented in Fig. 39), it is possible to compute the value of $R_{c,d}$ considering the base area of the triple element ($A_b = 4.32$ m²), the value of q_b at the foundation base ($q_b = 6.67$ MPa), the value of β according to equation (34) ($\beta = 0.94$). The design value of the base resistance of a triple CSM-bearing element is thus equal to 7287 kN (~730 tons per element).

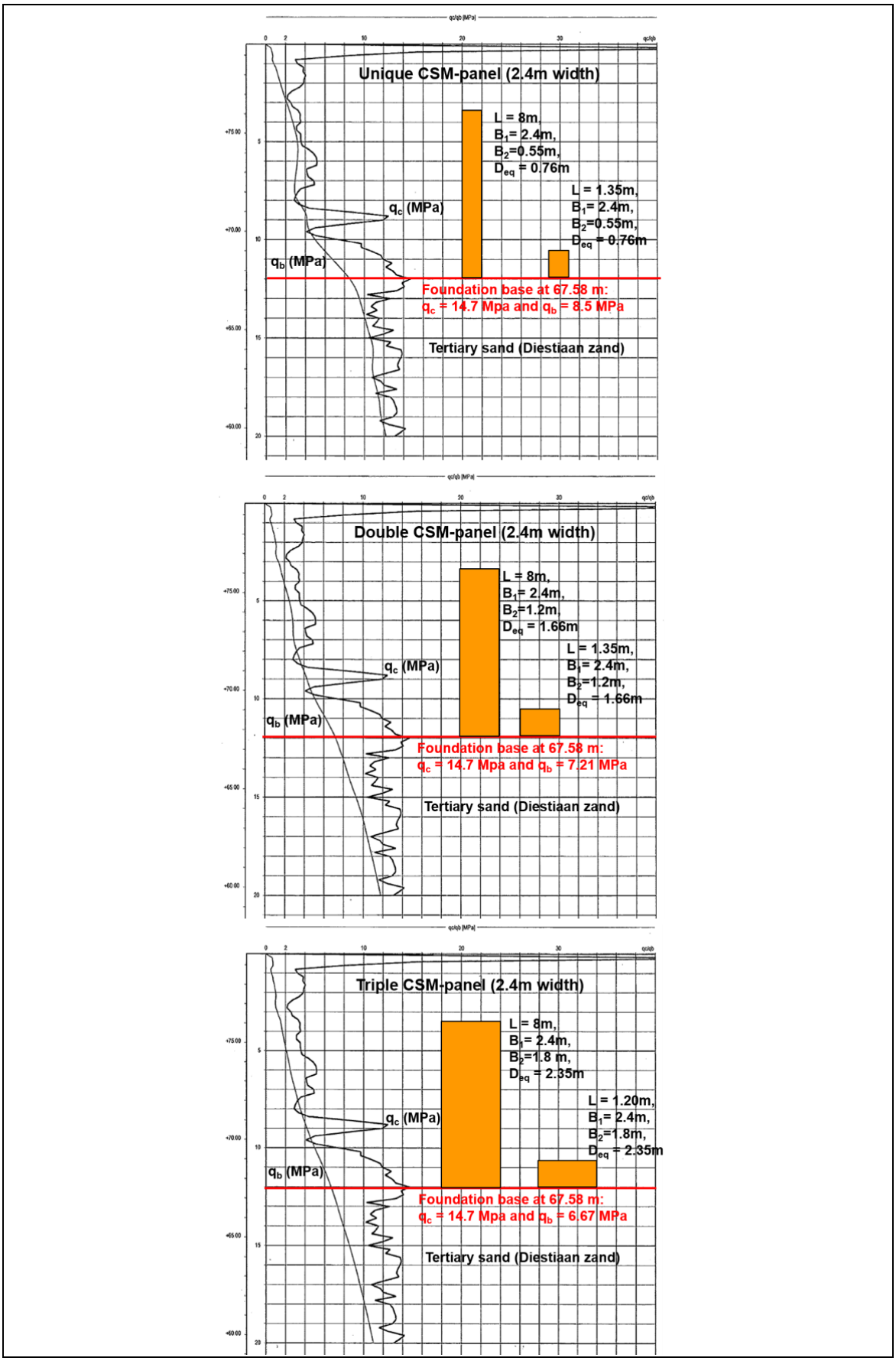

Figure 39: Different design configurations for the installation of the unique, double and triple CSM-panels, as installed on the construction site of the REGA-Instituut

Especially due to the importance of their base areas, the different CSM-bearing elements have brought a cost-effective solution to the design of the building foundations. Considering this case history, it is still possible to highlight the following discussion topics.

In this kind of design concept, the slabs under the building pillars are just installed on the top of the CSM-bearing elements. There is no load transfer platform foreseen to spread the stresses. That involves a direct transmission of the vertical (and potential lateral) loads on the top of the CSM-bearing elements. The compressive stresses will be therefore maximum at the top of the CSM-bearing elements. As a consequence, considering this kind of concept, it will be therefore necessary to provide a CSM-bearing element presenting a high quality material on the first meter. And this is not an easy task. Indeed, Ganne et al. (2010) have observed on different construction sites that the strength of the soil mix material over the first meter is strongly influenced by the execution process (e.g. infiltration of rinsing water and falls of lumps of earth in the fresh executed soil mix panel). With this kind of concept, a special attention has to be brought during the execution process to ensure a full-quality product on the first meter on the soil mix elements.

Another point of discussion concerns the geotechnical design of such kind of bearing elements. In the present case history, the CSM-bearing elements, formed of several CSM panels, have been computed as pile foundations only considering a base resistance and taking into account an installation factor ($\alpha_b = 0.5$) used for the bored piles according to the Rapport 12 of BBRI (Belgian National Annex of Eurocode 7 for piles).

One can still question that approach considering the dimensions of each CSM-bearing elements. Theoretically, considering its dimensions, a bearing element will respectively be computed as a shallow foundation, a pile foundation or a pier foundation (sometimes called "caissons"). Each type of foundation actually presents his own design approach corresponding to his own failure mechanism. And the value of the bearing capacity obtained with a design approach or another will sometimes lead to severe differences.

In Belgium, for example, according to the revised Rapport 12 of BBRI and the guidelines for shallow foundations (both in the pipeline for publication), a foundation element will be considered as

- a pile foundation as soon as the ratio pile length/diameter is larger than 5;
- a shallow foundation as soon as the ratio footing depth/width is smaller than 2.5;
- a pier foundation (generally called "puit" or "put" in Belgium) once the ratio footing depth/width is ranging between 2.5 and 5.

According to the Belgian National Annexes of Eurocode 7:

- The **foundation pile** will be computed according to the De Beer procedure based on the CPT results and particularly on the cone resistance.
- The design value of the bearing capacity of a **shallow foundation** will be computed considering the formulae (36) and (40) respectively in drained and undrained soil conditions.

  In drained conditions:

$$\frac{R_d}{A'} = c'N_c b_c s_c i_c g_c d_c + q'N_q b_q s_q i_q g_q d_q + \frac{1}{2}\gamma' B' N_\gamma b_\gamma s_\gamma i_\gamma g_\gamma d_\gamma \quad (36)$$

  where A' (m²) is the effective design surface of the foundation element and B' (m) is the effective width of the foundation element. c' (kPa) is the effective cohesion in drained conditions, q' (kPa) is the effective vertical design stress near the foundation at the foundation base and γ' (kN/m³) is the effective volumetric weight of the ground under the foundation. N_c, N_q and N_γ are the bearing capacity factors.

  According to Chen (1975), N_q and N_c can be defined as follows:

$$N_q = e^{\pi tan\varphi} tan^2\left(\frac{\pi}{4} + \frac{\varphi}{2}\right) \quad (37)$$

  and

$$N_c = (N_q - 1)cot\varphi \quad (38)$$

  and according to Eurocode 7, N_γ will be defined as:

$$N_\gamma = 2(N_q - 1)tan\varphi \quad (39)$$

  The factors b_c, b_q and b_g depend on the gradient of the foundation element. s_c, s_q and s_g are the form factors. i_c, i_q and i_g depend on the inclination of the load and the factors g_q, g_c and g_γ are given for an inclined ground surface. The d-factors are the footing depth factors of Meyerhof.

In undrained conditions:

$$\frac{R_d}{A'} = (\pi + 2)c_u b_c s_c i_c + q \quad (40)$$

where c_u (kPa) is the undrained cohesion.

- The bearing capacity of a **pier foundation** will be computed as the average of the two following values:
  - the bearing capacity of a shallow foundation using Meyerhof depth factors calculated for a ratio footing depth/width equal to 2.5;
  - the bearing capacity of a bored pile without shaft resistance.

If this is a clear computational procedure which allows to determine a bearing capacity for the three kinds of foundation generally considered in practice, the design procedure proposed for the pier foundations in the Belgian National Annex of Eurocode 7 mainly concerns the realization of foundations of intermediate dimensions ranging between the typical dimensions of a shallow foundation and a pile. The design of pier foundations of larger dimensions, as executed on the construction site of the REGA-Insituut, for example, could be regarded with a further attention. As illustrated in Fig. 39, on this construction site, the different CSM-bearing elements can be considered as pure shallow foundation (e.g. in the case of elements with L = 1.2 m and B_2 = 0.55 m; ratio = 2.1), as typical intermediate pier foundation (e.g. elements with L = 4.85 m and B_2 = 1.2 m; ratio = 4) and as pile foundation (e.g. elements with L = 8 m and B_2 = 0.55 m; ratio = 14.5).

Considering the CSM-bearing elements installed in triple configuration, the larger element presents the following dimensions: L = 8 m and B_2 = 1.8 m. This element will be considered as a pier foundation and its bearing capacity will be computed without taking into account the friction resistance arising along its shaft according to the Belgian National Annex of Eurocode 7. Nevertheless, considering the theory behind the drilled shaft foundations (presenting similar dimensions and installed with comparable method than the bored piles), the shaft resistance really plays an important role in the bearing capacity of such large bearing elements (Kulhawy, 1991). In the Foundation Engineering Handbook (1991), Kulhawy gives a methodology to design this kind of foundation. The particularities of this approach, well-adapted to deep foundations presenting a large diameter or large horizontal dimensions, are:
- the consideration of the weight of the foundation element in the design,
- the computation of the base resistance considering the bearing capacity equations (36) and (40) with potentially adapted bearing factors,
- the consideration of the side resistance.

In the case of the REGA-Instituut, a safety design approach was followed with success. But it will be really interesting in the future to monitor this kind of bearing element for the purpose of analysing the global behavior of the foundation with regard to the development of a shaft friction or not along the soil mix elements. Moreover, in this kind of hybrid foundation concept, with rigid inclusions but without a load transfer platform, the role of the surrounding soil in the design should be investigated. The way the load is transferred from the slab on grade or from the structure to the bearing elements and possibly to the surrounding soil has to be clarified.

To conclude this paragraph, it can be noted that the design of alternative bearing elements by the help of a particular design method should always be performed regarding the assumptions behind this design method; in particular considering the dimensions of the elements. A bearing element will often be designed as a shallow or a pile foundation only regarding the value of its dimensions. But a special attention should be brought to the use of a design method when these dimensions or the ratios between these dimensions are close to the boundaries of the field of application of the method. To complicate this issue, the boundaries between a pile, a pier or a shallow foundation (in terms of definitions) are often different between countries certainly involving a lack of clarity for the geotechnical designers playing with new alternative techniques such as the use of soil mix panels or columns as bearing elements.

6. CONCLUSION

A current trend on the European market is the use of ground improvement concepts as alternative to typical piling methods (e.g. the use of soil mix panels or columns as bearing elements in place of piles). The lack of design requirements concerning the ground improvement techniques was, for a long time, an obstacle to the development of such techniques on the European market - subjected to a strict control by means of the Eurocodes and the European standards - and sometimes leads to severe discussion between the GI contractors and the pile contractors denouncing a double standard politics on the foundation market. Nevertheless, this last decade, several design methods have been established for ground improvement techniques in line with the Eurocodes.

The present keynote concentrates on the presentation of the rigid inclusion concept involving the use of a load transfer platform and it particularly highlights the content of the ASIRI guidelines (IREX, 2012). The authors explain the failure mechanisms associated to this concept and the role of the load transfer platform considering the stress domain, the geotechnical and the structural limit states associated to the rigid inclusions. It is to note that the design of rigid inclusion concepts according to this approach falls within the philosophy of the Eurocodes.

The authors also refer to the Dutch guidelines (CUR rapport 226, 2010) involving the design of piled embankments and the installation of a geosynthetic reinforcement generally at the base of the load transfer platform. The consideration of these guidelines certainly provides an additional information to the geotechnical designer interested in the design of rigid inclusion concepts. Particular aspects which are deeply investigated in the Dutch approach are the design of the geosynthetic reinforcements installed at the base of this load transfer platform and the study of the load transfer distribution developing in this load transfer platform. The recent concentric arches model of Van Eekelen et al. (2013) is highlighted and the distribution of the line load on the reinforcement strip between two piles is discussed.

In the present keynote, the author focus on the use of rigid inclusions as an alternative to vertically loaded pile foundations. It can be noted that the design principles, presented in Section 2, can be extended to the application of lateral loads on the slabs on grade of the structure. Indeed, the load transfer platform will have a positive effect on the transmission of the lateral loads to the rigid elements.

Numerical modeling of the rigid inclusion concept is treated considering the guidelines of IREX (2012) underlining the relevant parameters and assumptions to be used for the modeling. Advantages and drawbacks of the 2D- and 3D-modeling are discussed regarding the complexity of the design. A particularity of the numerical methods modeling the rigid inclusion solutions is the consideration of the inclusion/soil interface. As reported in IREX (2012), the constitutive models typically used for interfaces are elastoplastic. The elastic part allows the modeling of a progressive mobilization of the shear with strain. As for the plastic part, the authors report the recent work of Racinais (2015) who models a fictitious soil with $\phi' = 0$ and with a nonzero cohesion for simulating constant friction $c'=q_s$, in compliance with the limiting values of shaft friction set forth by the French standard for deep foundations NF P 94-262. Racinais (2015) calibrates the soil parameters of a rigid inclusion problem on the Frank and Zhao friction curves (1982) in order to obtain better simulations of the rigid inclusion behavior with the help of the Plaxis software for a practical case.

After design considerations, the authors review several execution techniques allowing the installation of rigid inclusions and they focus on impressive case histories illustrating the realization of Controlled Modulus Columns (CMCs) at large depths in USA.

In the last part of the keynote, the authors finally report a case history in Leuven (Belgium), where CSM-panels were used as soil mix bearing elements as an alternative to pile groups to support the pillars of an eleven story-building. The design of these CSM-bearing elements is discussed regarding the nature of the bearing elements and their dimensions. Structural and geotechnical designs are both considered in line with the principles of Eurocode 7. A particular attention is given to the suitability of a design method with regard to the dimensions of the bearing elements.

If the use of rigid inclusions in combination with a load transfer platform is now well-established, the hybrid foundation concept, such as presented in the last part of the keynote, with the use of CSM-panels in place of pile groups has to be more deeply investigated. In this concept, no load transfer platform is used to transfer the structural loads to the foundation elements. The soil has probably (?) no more any role in the bearing capacity and in the mitigation of the settlement contrarily to the concept of the rigid inclusions with a load transfer platform. Further research has to be conducted to investigate the real behavior of such bearing elements in the ground (in particular with regard to the shaft resistance).

In the case of the REGA-Instituut, the CSM-panels were not reinforced with the help of steel beams; only vertical loads applying on the top of the CSM-bearing elements. Nevertheless, the reader can refer to the SBRCURnet/BBRI soil mix handbook (2016) to obtain more information on the design requirements of soil mix elements used with a bearing function. In this handbook, the design of the bearing capacity of the soil mix element is detailed according to a procedure in line with Eurocode 7 and requirements are given for the corrosion protection of the steel beams in agreement with the content of the EN 1993-5 for the piles.

The respect of guidelines (IREX, 2012; CUR-rapport 226, 2010; SBRCURnet/BBRI soil mix handbook, 2016…) in line with the Eurocodes should lead to a growing and sustainable use of alternative ground improvement techniques on the market with a positive competition between the techniques and the contractors.

In order to conclude, if ground improvement and piling techniques are often used in competition, geotechnical designers begin to use them in combination. Indeed, we move towards geotechnical designs more and more based on the functions and lifetime of each geotechnical element combining them to reach an optimized design. For example, in 2013, Yamashita et al. report measurements performed underneath a piled raft completed with grid-form deep cement mixing walls installed to reduce the risks of structural damages potentially caused by liquefaction in case of earthquake. The structure was a twelve-storey office building. Figure 40 presents a schematic view of the building and foundation. Figure 40 illustrates the layout of piles and grid-form deep cement mixing walls. The load distribution between the piles, the soil mix walls and the surrounding soil has been monitored during a period of three years. As a result of the monitoring measurements, 70 % of the load was taken by the piles, 14 % by the soil mix walls and 15% by the soil. A settlement of 20 mm was observed after three years of monitoring. The measurements also learned that the magnitude 9.0 Tohoku earthquake (on March 11, 2011) had almost no influence on the settlements and on the load distribution. As for this case, it is certain that in a near future, the combination of ground improvement with typical piling techniques will be more and more regarded in view of optimizing design and costs of construction project.

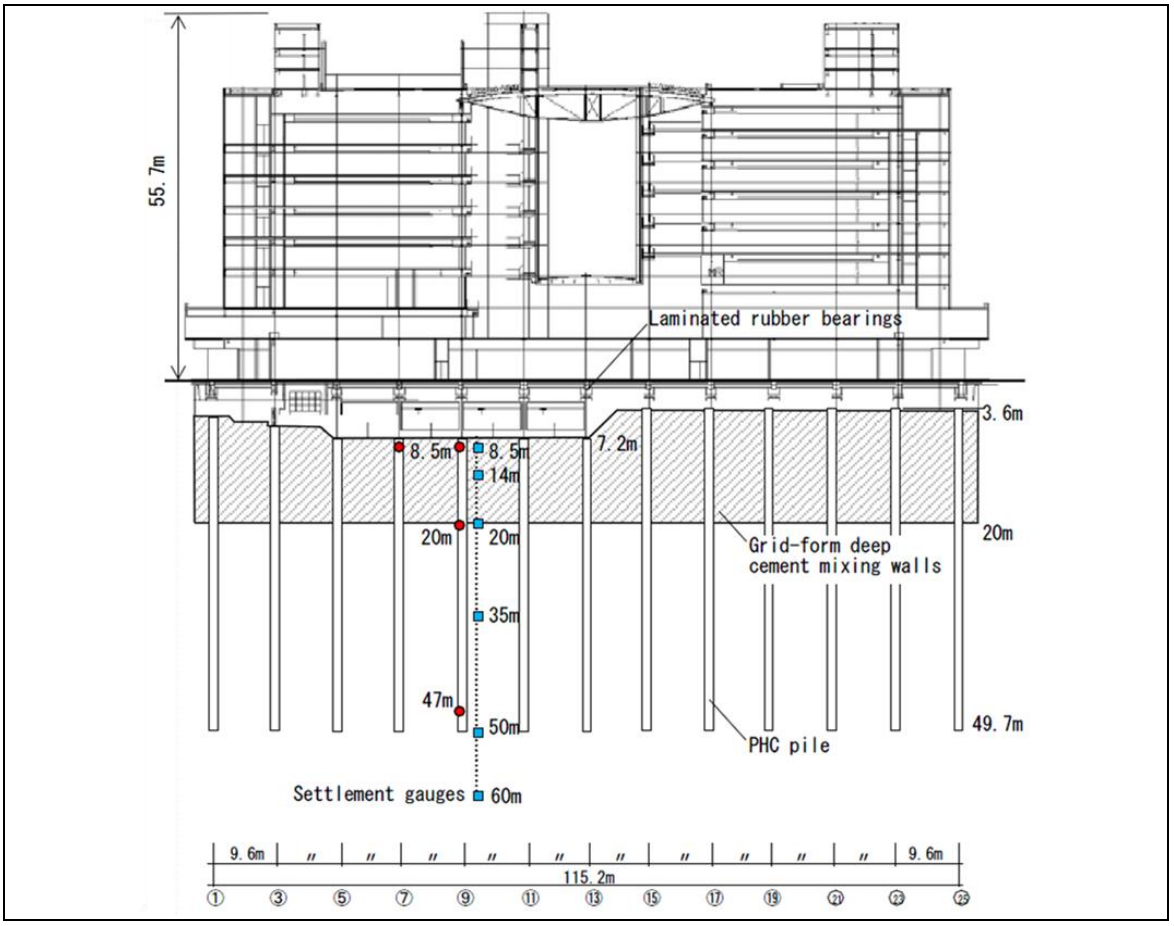

Figure 40: Schematic view of the building and foundation (Yamashita et al., 2013)

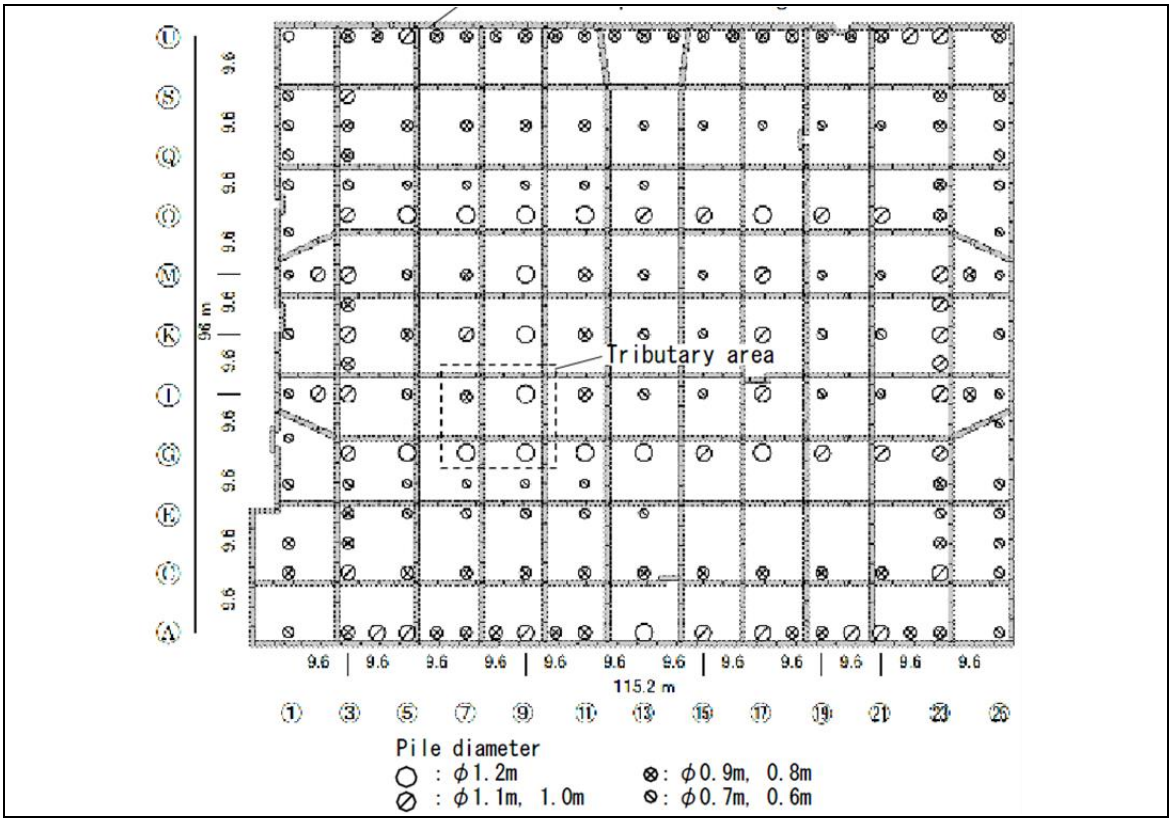

Figure 41: Layout of piles and grid-form deep cement mixing walls (Yamashita et al., 2013)

REFERENCES

Aboshi, H., Ichimoto, E. & Harada, K. 1979. The Compozer: A Method to Improve Characteristics of Soft Clays by Inclusion of Large Diameter Sand Columns. International Conference on Soil Reinforcement; Reinforced Earth and Other Techniques, 2, Paris, 20-22 March, 211–216

ALLU. 2010. Mass Stabilisation Manual, ALLU Finland Oy

American Petroleum Institute. 2001. API Standard 653: Tank Inspection, Repair, Alteration, and Reconstruction, 3rd Edition, 112

Barksdale, R. D., and Bachus, R. C. 1983. "Design and Construction of Stone Columns, Volume 1, FHWA/RD-83/026." 194

BBRI CSTC WTCB. 2009. Rapport 12. Directives pour l'application de l'Eurocode 7 en Belgique. Partie 1 : dimensionnement géotechnique à l'état limite ultime de pieux sous charge axiale de compression. Richtlijnen voor de toepassing van de Eurocode 7 in België. Deel 1: het grondmechanische ontwerp in de uiterste grenstoestand van axiaal op druk belaste funderingspalen

BBRI Soil Mix project. 2009-2013. IWT 080736 soil mix project. SOIL MIX in constructieve en permanente toepassingen – Karakterisatie van het materiaal en ontwikkeling van nieuwe mechanische wetmatigheden. See Denies et al. (2012) for more information

Bruce, D. A., Bruce, M. E. C. and DiMillio, A. F. 1998. Deep mixing method: a global perspective. ASCE, Geotechnical special publication, n°81, pp. 1-26

Bowles, J. E. 1996. Foundation Analysis and Design, 5th Ed., New York, McGraw Hill, 1175

BS 8006-1. 2010. Code of practice for strengthened/reinforced soils and other fills

Burke G.K. 2012. The State of Practice of Jet Grouting. ASCE Geotechnical Special Publication No. 228. Proceedings of the 4th Interantional Conference on Grouting and Deep Mixing. Pp. 74-88

Buschmeier, B., Masse, F., Swift, S. & Walker, M. 2012. Full Scale Instrumented Load Test for Support of Oil Tanks on Deep Soft Clay Deposits in Louisiana Using Controlled Modulus Columns. International Symposium on Ground Improvement (IS-GI) Brussels 2012, 3, Brussels, 31 May - 1 June, 359-372

Burland, J. B. 1973. Shaft Friction Piles in Clay - a Simple Fundamental Approach. Ground Engineering, 6, 3, 30-42

Caquot A., Kerisel J. 1966. Traité de mécanique des sols, Gautier-Villars

Cartiaux F.-B., Gellee A., Buhan (de) P., Hassen G. «Modélisation multiphasique appliquée au calcul d'ouvrages en sol renforcé par inclusions rigides ». Revue française de géotechnique, n° 118, 2007, p. 43-52.

CDIT. Coastal Development Institute of Technology. 2002. The Deep Mixing Method – Principle, Design and Construction. Edited by CDIT, Japan. A. A. Balkema Publishers/Lisse/Abingdon/Exton (PA)/Tokyo

Chen, W. F. 1975. Limite analysis and soil plasticity, Elsevier, Amsterdam.

Chu, J., Varaksin, S., Klotz, U. & Mengé, P. 2009. State of the Art Report: Construction Processes. 17th International Conference on Soil Mechanics & Geotechnical Engineering: TC17 meeting ground improvement, Alexandria, Egypt, 7 October 2009, 130

Combarieu, O. 1988. Amélioration des sols par inclusions rigides verticales. Application à l'édification de remblais sur sols médiocres. Revue Française de Géotechnique, 44, 57-79

Croce, P., Flora, A. & Modoni, G. (2014). Jet Grouting Technology, Design and Control, CRC Press, Taylor & Francis Group.

Cuira F., Simon B. 2009. Deux outils simples pour traîter des interactions complexes d'un massif renforcé par inclusions rigides. Proc. 17th ICSMGE, Alexandrie, M. Hamza et al. (Eds.), IOS Press, 2009, p. 1163-1166.

CUR-rapport 226. 2010. Ontwerprichtlijn paalmatrassystemen.

Das, B. M. 2009. Shallow Foundations Bearing Capacity and Settlement, 2nd Ed, Boca Raton, FL, USA, Taylor & Francis Group.

Denies, N., Huybrechts, N., De Cock, F., Lameire, B., Vervoort, A., Van Lysebetten, G. and Maertens, J. 2012. Soil Mix walls as retaining structures – mechanical characterization. International symposium of ISSMGE - TC211. Recent research, advances & execution aspects of ground improvement works. 31 May-1 June 2012, Brussels, Belgium

Denies, N. and Van Lysebetten, G. 2012. General report Session 4 – Soil Mixing 2 – Deep Mixing. Proceedings of the International symposium of ISSMGE - TC211. Recent research, advances & execution aspects of ground improvement works. N. Denies and N. Huybrechts (eds.). 31 May-1 June 2012, Brussels, Belgium, Vol. I, pp. 87-124

Denies, N., Van Lysebetten, G., Huybrechts, N., De Cock, F., Lameire, B., Maertens, J. and Vervoort, A. 2013. Design of Deep Soil Mix Structures: considerations on the UCS characteristic value. Proceedings of the 18th International Conference on Soil Mechanics and Geotechnical Engineering, Paris, France, 2013, Vol. 3, pp. 2465-2468

Denies, N., Van Lysebetten, G., Huybrechts, N., De Cock, F., Lameire, B., Maertens, J. and Vervoort, A. 2014. Real-Scale Tests on Soil Mix Elements. Proceedings of the International Conference on Piling & Deep Foundations, Stockholm, Sweden, 21-23 May 2014, Eds. DFI & EFFC, pp. 647-656

Denies, N. and Huybrechts, N. 2015. Deep Mixing Method – Equipment and Field of Applications, Chapter 11 of the book: Ground Improvement Case Histories. Elsevier

DIN 4093. 2012. Design of ground improvement – Jet grouting, deep mixing or grouting. August 2012

EBGEO. 2011. Recommendations for Design and Analysis of Earth Structures using Geosynthetic Reinforcements – EBGEO. Ernst & Sohn – A Wiley company. DGGT - Deutsche Gesellschaft für Geotechniek e. V. - German Geotechnical Society

EN 206. 2013. Concrete – Part 1: Specification, performance, production and conformity

EN 1536. 2015. Execution of special geotechnical work - Bored piles

EN 1992-1-1. 2004. Eurocode 2: Design of Concrete Structures – Part 1-1: General – Common Rules for Building and Civil Engineering Structures

EN 1993-5. 2007. Eurocode 3: Design of steel structures - Part 5: Piling

EN 1997-1. 2004. Eurocode 7: Geotechnical Design - Part 1: General Rules 1

Essler and Shibazaki. 2004. Jet grouting. In M. P. Moseley & K. Kirsch (Eds.), Ground improvement, 2nd ed., Spon Press

Essler, R. and Kitazume, M. 2008. Application of Ground Improvement: Deep Mixing. TC17 website: www.tc211.be

Eurocode 2 – see reference EN 1992-1-1

Eurocode 7 – see reference EN 1997-1

Eurosoilstab. 2002. Development of design and construction methods to stabilise soft organic soils. Design Guide Soft Soil Stabilisation. EC project BE 96-3177

FHWA-RD-99-167. 2001. An introduction to the Deep Soil Mixing Methods as used in geotechnical applications: verification and properties of treated soil. Prepared by Geosystems (D.A. Bruce) for US Department of Transportation, FHWA, p. 434

FHWA-HRT-13-046. 2013. Federal Highway Administration Design Manual: Deep Mixing for Embankment and Foundation Support. US Department of Transportation, Federal Highway Administration, October 2013, p. 244

Frank, R. & Zhao, S. R. 1982. Estimation Par Les Parametres Pressiometriques de 1'enfoncementt Sous Charge Axiale de Pieux Fores dans des Sols Fins. Bulletin Laison Laboratoire Central des Ponts et Chaussees, 119, 17-24.

Ganne, P., Huybrechts, N., De Cock, F., Lameire, B. & Maertens, J. 2010. Soil mix walls as retaining structures – critical analysis of the material design parameters, Geotechnical challenges in megacities. International Geotechnical Conference, Moscow, Vol. 3, pp. 991-998.

Geotech Tools. 2013. Geo-construction Information & Technology Selection Guidance for Geotechnical, Structural, & Pavement Engineers. 2013. http://geotechtools.org/ Copyright © 2010–2013 Iowa State University

Hamidi, B., Masse, F., Racinais, J. & Varaksin, S. (in print) The Boundary between Deep Foundations and Ground Improvement. Geotechnical Engineering.

Hamidi, B., Nikraz, H., and Varaksin, S. 2009. "Arching in Ground Improvement." Australian Geomechanics Journal, 44(4 (December)), 99-108.

Hansen, J. B. 1970. A Revised and Extended Formula for Bearing Capacity. Danish Geotechnical Institute Bulletin, 28 (successor to Bulletin No 11), 21.

Hassen G., Dias D., Buhan (de) P. 2009. Multiphase constitutive model for the design of piledembankments: comparison with three-dimensional numerical simulations. International Journal of Geomechanics, vol. 9, n° 6, 2009, p. 258-266.

Holm, G. 2000. Deep Mixing. ASCE, Geotechnical special publication, N°112, pp. 105-122

IREX. 2012. Recommandations pour la conception, le dimensionnement, l'exécution et le contrôle de l'amélioration des sols de fondation par inclusions rigides (for the French version). Recommendations for the design, construction and control of rigid inclusion ground improvements (for the English version). Projet National ASIRI. Presses des Ponts, ISBN 978-2-85978-462-1 (available in French and English).

Kitazume, M. and Terashi, M. 2013. The Deep Mixing Method. CRC Press/Balkema. Taylor and Francis Group, London, UK

Kulhawy, F. H. 1991. Drilled shaft foundations. Chapter 14 of the Foundation Engineering Handbook, second edition. Van Nostrand Reinhold.

Larsson, S.M. 2005. State of practice report - Execution, monitoring and quality control, International Conference on Deep Mixing, pp. 732-785

Lawson, C.R. 2012. Role of Modelling in the Development of Design Methods for Basal Reinforced Piled Embankments, Proceedings of EuroFuge 2012, Delft, the Netherlands.

Le Hello, B., Villard, P. 2009. Embankments reinforced by piles and geosynthetics - numerical and experimental studies with the transfer of load on the soil embankment. Engineering Geology 106, 78-91.

Liu, H.L. 2007. New piling techniques for soil improvement in China, Proc 13 Asian Regional Conf on Soil mech and Geot Eng. Kolkata.

Maertens, J., De Vleeschauwer, P. and Langhorst, O. 2016. Jet grouting: State of the Art.

Masse, F., Pearlman, S. L. & Taube, M. G. 2009. Controlled Modulus Columns for Support of above Ground Storage Tanks. 40th Ohio River Valley Soil Seminar (ORVSS), Lexington, Kentucky, November 13.

Meyerhof, G. G. 1951. The Ultimate Bearing Capacity of Foundations. Geotechnique, 2, 4, 301-333.

Murayama, S. 1962. Vibro-Compozer Method for Clayey Ground (in Japanese). Mechanization of Construction Work, 150, 10-15.

NF P 94-262. 2012. Justification des ouvrages géotechniques. Norme d'application nationale de l'Eurocode 7 - Fondations profondes.

Okyay, U. S. 2010. Etude expérimentale et numérique des transferts de charge dans un massif renforcé par inclusions rigides. Application à des cas de chargements statiques et dynamiques. Civil and Environmental Engineering. Lyon, Institut National des Sciences Appliquées de Lyon, 402.

Porbaha, A. 1998. State of the art in deep mixing technology: part I. Basic concepts and overview. Ground Improvement, Vol. 2, pp. 81-92

Prandtl, L. 1920. Uber Die Härte Plastischer Körper Nachrichten Von Der Königlichen Gesellschaft Der Wissenschaften, Gottingen, Math.- Phys. Klasse, pp. 74-85.

Racinais, J. 2015. Calibration of Rigid Inclusion Parameters Based on Pressuremeter Test Results. 16th European Conference on Soil Mechanics and Geotechnical Engineering (XVI ESCMGE), Edinburgh, 13-17 September, Presentation.

Rutherford, C., Biscontin, G. and Briaud, J.-L. 2005. Design manual for excavation support using deep mixing technology. Texas A&M University. March 31, 2005

Salgado, R. 2008. The Engineering of Foundations. McGraw-Hill International Edition.

SBRCURnet/BBRI. 2016. Soilmix-handboek [in Dutch].

Schweiger, H. F. 2002. Results from Numerical Benchmark Exercises in Geotechnics. 5th European Conference Numerical Methods in Geotechnical Engineering (NUMGE 2002), Paris, 4-6 September, 305-314.

Shibazaki, M. 2003. State of Practice of Jet Grouting. ASCE Geotechnical Special Publication No. 120. Proceedings of the Third International Conference on Grouting and Ground Treatment, pp. 198-217.

Slaats, H. and van der Stoel, A.E.C. 2009. Validation of numerical model components of LTP by means of experimental data. Proceedings of the 17th International Conference on Soil Mechanics and Geotechnical Engineering (ICSMGE 2009).

Sudret B., Buhan (de) P. 2001. Multiphase model for inclusion-reinforced geostructures. Applications to rock-bolted tunnels and piled raft foundations. International Journal for Numerical and Analytical Methods in Geomechanics, vol. 25, 2001, p. 155-182.

Thai Son Q., Hassen G., Buhan (de) P. 2009. Dimensionnement sous sollicitation sismique de sols de fondations renforcés par inclusions rigides. Proc. 17th ICSMGE, Alexandrie, M. Hamza et al. (Eds.), IOS Press, 2009, p. 606-609.

Thai Son Q., Hassen G., Buhan (de) P. 2010. Seismic stability analysis of piled embankments: a multiphase approach. International Journal for Analytical and Numerical Methods in Geomechanics, vol. 34, 2010, p. 91-110.

Terashi, M. 2003. The State of Practice in Deep Mixing Methods. Grouting and Ground Treatment (GSP 120), 3rd International Specialty Conference on Grouting and Ground Treatment New Orleans, Louisiana, USA, pp. 25-49

Terzaghi, S. 1943. Theoretical Soil Mechanics, New York, John Wiley & Sons, 510.

Terzaghi, K., Peck, R. B. & Mesri, G. 1996. Soil Mechanics in Engineering Practice, 3rd Edition, New York, John Wiley and Sons, 512.

Tomlinson, M. J. 1971. Some Effects of Pile Driving on Skin Friction. Conference on Behaviour of Piles, London, 107-114.

Topolnicki, M. 2004. In situ soil mixing. In M. P. Moseley & K. Kirsch (Eds.), Ground improvement, 2nd ed., Spon Press

Topolnicki, M. and Pandrea, P. 2012. Design of in-situ soil mixing. International symposium of ISSMGE - TC211. Recent research, advances & execution aspects of ground improvement works. 31 May-1 June 2012, Brussels, Belgium

Van Eekelen, S.J.M.; Bezuijen, A. and Van Tol, A.F., 2011. Analysis and modification of the British Standard BS8006 for the design of piled embankments. Geotextiles and Geomembranes 29 (2011) pp.345-359.

Van Eekelen, S.J.M. and Bezuijen, A. 2012. Basal reinforced piled embankments in the Netherlands, Field studies and laboratory tests. International symposium of ISSMGE - TC211. Recent research, advances & execution aspects of ground improvement works. 31 May-1 June 2012, Brussels, Belgium

Van Eekelen, S.J.M., Bezuijen, A., van Tol, A.F., 2013. An analytical model for arching in piled embankments. Geotext. Geomemb. 39, 78-102.

Vijayvergiya, V. N. & Focht, J. A. 1972. A New Way to Predict Capacity of Piles in Clay. 4th Offshore Technology Conference, Houston, paper 1718.

Yamashita, K., Wakai, S. & Hamada, J. 2013. Large-scale piled raft with grid-form deep mixing walls on soft ground. 18th International Conference on Soil Mechanics and Geotechnical Engineering, 2-6 September, Paris, Vol. 3, pp. 2637-2640.

Zaeske, D., 2001. Zur Wirkungsweise von unbewehrten und bewehrten mineralischen Tragschichten über pfahlartigen Gründungselementen. Schriftenreihe Geotechnik, Uni Kassel, Heft 10, February 2001 (in German).